AD_____

Award Number: DAMD17-03-1-0616

TITLE: Transcription Factor Stat5, A Novel Therapeutic Protein, Inhibits Metastatic Potential and Invasive Characteristics of Human Breast Cancer Cells

PRINCIPAL INVESTIGATOR: Ahmed S. Sultan, Ph.D.

CONTRACTING ORGANIZATION: Georgetown University Medical Center
Washington, DC 20007

REPORT DATE: October 2004

TYPE OF REPORT: Final

PREPARED FOR: U.S. Army Medical Research and Materiel Command
Fort Detrick, Maryland 21702-5012

REPORT DOCUMENTATION PAGE

Form Approved
OMB No. 074-0188

1. AGENCY USE ONLY (Leave blank)	2. REPORT DATE	3. REPORT TYPE AND DATES COVERED
	October 2004	Final (30 Sep 2003 - 29 Sep 2004)

4. TITLE AND SUBTITLE
Transcription Factor Stat5, A Novel Therapeutic Protein, Inhibits Metastatic Potential and Invasive Characteristics of Human Breast Cancer Cells

5. FUNDING NUMBERS
DAMD17-03-1-0616

6. AUTHOR(S)
Ahmed S. Sultan, Ph.D.

7. PERFORMING ORGANIZATION NAME(S) AND ADDRESS(ES)
Georgetown University Medical Center
Washington, DC 20007

E-Mail: Ass6@georgetown .edu

8. PERFORMING ORGANIZATION REPORT NUMBER

9. SPONSORING / MONITORING AGENCY NAME(S) AND ADDRESS(ES)
U.S. Army Medical Research and Materiel Command
Fort Detrick, Maryland 21702-5012

10. SPONSORING / MONITORING AGENCY REPORT NUMBER

11. SUPPLEMENTARY NOTES
Original contains color plates: All DTIC reproductions will be in black and white.

12a. DISTRIBUTION / AVAILABILITY STATEMENT
Approved for Public Release; Distribution Unlimited

12b. DISTRIBUTION CODE

13. ABSTRACT (Maximum 200 Words)

Signal transducer and activator of transcription-5 (Stat5) mediates prolactin (PRL)-induced differentiation and growth of breast epithelial cells. We have recently identified active Stat5 as tumor marker of favorable prognosis in human breast cancer, and determined that Stat5 activation is lost during metastatic progression. Here we provide novel evidence for an invasion-suppressive role of Stat5 in human breast cancer. Activation of Stat5 by PRL in human breast cancer lines was associated with increased surface levels of the invasion-suppressive adhesion molecule, E-cadherin, *in vitro* and in xenotransplant tumors *in vivo*. Inducible E-cadherin was blocked by dominant-negative (Dn) Stat5 or Dn-Jak2, but not by Dn-Stat3. Further experimental data indicated a role of Stat5 as a coordinate regulator of additional invasion-related characteristics of human breast cancer cells, including cell surface-association of β-catenin, homotypic cell clustering, invasion through Matrigel, cell migration, and matrix metalloproteinase activity. A role of Stat5 as a suppressor of breast cancer invasion and metastatic progression provides a biological mechanism to explain the favorable prognosis associated with active Stat5 in human breast cancer.

14. SUBJECT TERMS
Stat5, breast cancer, invasion, adhesion, motility, metastasis

15. NUMBER OF PAGES
31

16. PRICE CODE

17. SECURITY CLASSIFICATION OF REPORT	18. SECURITY CLASSIFICATION OF THIS PAGE	19. SECURITY CLASSIFICATION OF ABSTRACT	20. LIMITATION OF ABSTRACT
Unclassified	Unclassified	Unclassified	Unlimited

Table of Contents

Cover.....

SF 298.....

Table of Contents.....

Introduction.....1

Body.....2

Key Research Accomplishments.....10

Reportable Outcomes.....10

Conclusions.....10

References.....11

Appendices.....13

Transcription Factor Stat5, A Novel Therapeutic Protein, Inhibits Metastatic Potential And Invasive Characteristics of Human Breast Cancer Cells.

Final Report by PI: Ahmed S. Sultan, M.MS, Ph.D.
Georgetown University Medical Center, Lombardi Cancer Center

INTRODUCTION

A. Specific Aims and Significance of Proposed Research: About one woman in every nine can expect to develop breast cancer in her lifetime. Breast cancer is the most common cancer among women in the U.S., with an annual incidence of about 203,500 new cases, and leading to 39,600 deaths per year. In the U.S. population alone, approximately two million women have been diagnosed with breast cancer at some point in their lives (1, 2).
The vast majority of breast cancer fatalities result from metastatic spread of the primary tumor. Nonetheless, the formation of metastases remains a poorly understood and complex process. Identifying the early molecular changes that promote metastatic progression of breast cancer is needed for better therapeutic intervention of advanced breast cancer and better treatment for patients. As an outcome of the proposed investigations, we expect to identify the role of Stat5 as a novel suppressor of invasive characteristics of breast cancer, which in turn leads to determine the early molecular changes that promote metastatic progression of breast cancer.

Our **long-range goal** is to identify the molecular mechanisms of breast cancer progression from solitary tumor to metastasis. We place special emphasis on the early molecular events involved in the epithelial-to-mesenchymal dedifferentiation that is required for migration of individual tumor cells and establishment of metastatic cell colonies. Based on our extensive molecular analysis of clinical human breast cancer specimens and a series of experimental breast cancer models, we now present novel data that support a critical role for the transcription factor Stat5 in suppressing early invasion of human breast cancer. Specifically, we have tested the following ***central hypothesis***: Our ***working hypothesis*** is that Stat5 maintains homotypic adhesion of a majority of human breast cancer cells by preserving normal E-cadherin/β-catenin complexes, and inhibits the invasive characteristics of tumor cells. Stat5 activity has been experimentally manipulated in human breast cancer cells for *in vitro* studies of invasion and *in vivo* studies of peritumoral stromal invasion and metastasis in nude mice using a series of molecular tools that we have generated. These tools include viral and non-viral delivery of: a) wild-type (Wt) and dominant-negative (Dn) mutants of Stat5, b) Wt and Dn mutants of the Stat5 tyrosine kinase, Jak2, and c) antisense methodology for proven, effective suppression of Jak2.

B. Specific Goal:
The target of this project is to identify the mechanistic role for Stat5 as an important gatekeeper for metastasis by maintaining cell differentiation in human breast epithelial cells. We have been working towards this goal by completing the following specific aims:

Specific aim 1) Establish whether Stat5 stimulates human breast cancer cell differentiation and adhesion, and suppresses tumor cell invasion, in vitro and in vivo.
Specific aim 2) Determine the effect of activated Stat5 on invasion and metastasis of mouse breast cancer models in vivo.

C. Main Accomplishments

1-Novel progress supporting a role for Stat5 in maintaining homotypic cell adhesion of human breast cancer cells.

Functional validation of our new dominant-negative Stat5 adenoviral construct.

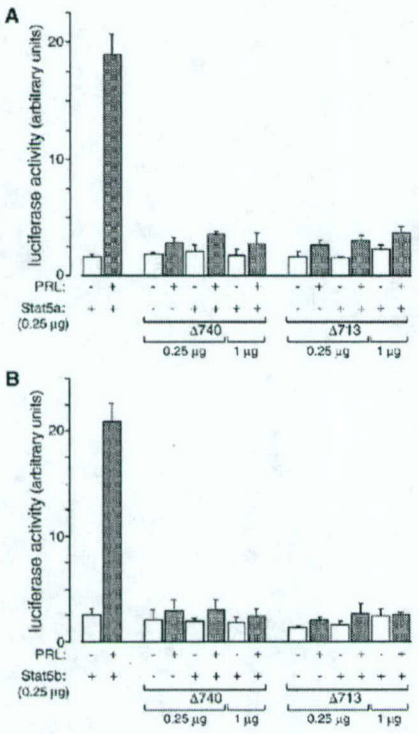

As one approach to experimentally block function of Stat5, we have generated and functionally tested two DN Stat5 constructs that lack transcriptional activation domain and effectively block both Stat5a and Stat5b (Fig. 1). We have proceeded to clone both into adenoviral vectors and purified functional virus stocks, and demonstrated that human breast cancer cells are receptive to adenoviral gene delivery (Fig. 2). As shown in Fig. 2, we have validated prolonged expression of DN-Stat5 delivered by adenovirus into human breast cancer cells. Stat5-DN protein levels expressed in MCF-7 cells 2 days after a 90 min infection period was dose-dependent (Fig. 2A).

Fig. 1. Both Δ740 and Δ713 Dominant-negative Stat5 completely inhibit Prl-induced Stat5a (top) and Stat5b (bottom) activity. A Stat5 sensitive β-casein promoter linked to a luciferase reporter gene was used.

Stimulation with 10 nM PRL for 30 min specifically induced tyrosine phosphorylation of Stat5-DN, suggesting that the protein will only be activated under conditions where Stat5 is normally activated. Protein levels were maintained at least for 5 days after initial infection. We extended this analysis to show that DNA binding of Stat5-DN is induced by serum and by PRL on day 2 as well as on day 5 after the infection (Fig. 2B).

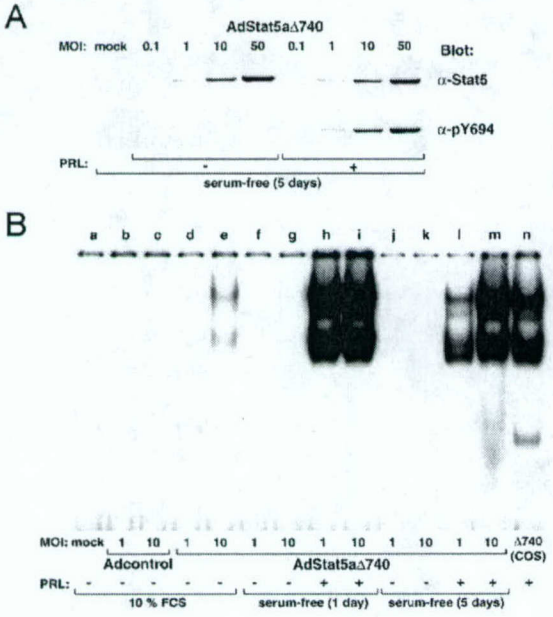

Fig. 2. Adenoviral delivery of Dn-Stat5a Δ740. Protein levels correspond to increasing MOI, and retain Prl-inducibility as illustrated by tyrosine phosphorylation immunoblotting (A). Δ740 Stat5a also binds DNA when stimulated by Prl as shown by EMSA (B), even 5 days after single exposure to virus. AdStat5aΔ713 is equally effective (not shown). We have proceeded to generate AdStat5-wt as a control, and AdStat5-Y694F dead (inactive) mutant, so we have a complete set of controls. Combined with our published Ad-Jak2-Wt and Ad-Jak2-Dn (3), we have a solid battery of viral gene delivery tools for suppression of Stat5 activity.

2-Generation of novel mouse model for controlled inhibition of Stat5 activation in established mammary tumors.

Description of mouse model:

As one strategy to inhibit Stat5 activation in mouse tumors, the Co-PI, Dr Wagner, has generated a conditional knockout allele of the *Jak2* gene that will allow us to genetically switch off Jak2-Stat5 signaling in any given cell of the organism, at any given time point, and at any given physiological stage including neoplastic transformation.

Generation of genetically engineered mice with a conditional knockout allele of the *Jak2* gene: We have described earlier in detail the strategy of how to establish a conditional knockout mouse (4). Following two steps were performed to generate the *Jak2* conditional knockout mice:

Step I: Cloning of the Jak2 gene and construction of the targeting vector. A BAC clone encompassing the *Jak2* locus was isolated from a mouse 129/SvJ genomic library. A 5.1 kb *Eco*RI fragment harboring the first coding exon, and a 5'- overlapping 5.2 kb *Hin*DIII fragment were isolated and cloned into pBluescript. Both clones were sequenced and used as a template to generate the *targeting vector* for the introduction of loxP sites into the endogenous *Jak2* locus. The entire *Hin*DIII fragment was released by *Asp*I and *Bam*HI digestion and cloned into pLoxpNeo upstream of the PGK-neomycin cassette. A 1.3 kb fragment with the first coding exon was amplified by Pfx polymerase, introducing a *Xho*I site on the 5'-end of the amplification product. The PCR fragment was cloned blunt into the *Hin*DIII(blunt) site 5' of the single loxP site of vector pBS64 (a kind gift from Ed Rucker, Univ. of Missouri). A second 3.1 kb Pfx PCR fragment containing a *Not*I site at the 3' end was cloned 3' of the loxP site into pBS64. The PCR product was cloned blunt into the *Eco*RV site of pZErO and released by *Eco*RI digest. The fragment was then cloned into the *Eco*RI site of the pBS64 vector, 3' from the loxP site. The entire 4.4 kb fragment was released from the pBS64 vector by *Xho*I/*Not*I and subcloned into the pLoxpNeo vector containing the 5.2 kb 5' homology region. The final targeting construct contained a floxed PGK-neomycin selection marker approximately 570 bp upstream and a third loxP site 450 bp downstream of the first coding exon. The gene-targeting vector was sequenced, and the functionality of each of the loxP sites was tested in AM-1 cells (Invitrogen) that express Cre recombinase.

Step 2: Gene targeting in embryonic stem (ES) cells and generation of Jak2 floxed mice. The gene-targeting vector was linearized using *Not*I and electroporated into isogenic RW-4 ES cells. Analysis of G418-resistant clones by Southern blot using *Eco*R1 as a restriction enzyme and a 3' diagnostic probe outside of the targeting region (Fig. 14) indicated that about 6% (12/192) of the ES cell clones had undergone correct homologous recombination. The recombination event on the 5' end was verified using a Southern blot strategy with *Eco*RV as restriction enzyme. Three of the twelve correctly targeted ES cell clones (#2, #88, and #190) were expanded and injected into C57/Bl6 blastocysts. The blastocyst injections were done as a subcontract by Cell & Molecular Technologies, Inc. Germline transmission of the *Jak2* floxed allele was achieved from male chimeras, and mice of line #88 were used for conditional knockout experiments. We then developed various PCR assays for identification of the wild type, floxed, and knockout alleles of the *Jak2* gene. The following primer pair can discriminate the wild type allele (230 bp) from the floxed locus (310 bp): #1743 (5'-ATT CTG AGA TTC AGG TCT GAG C-3') and #1744 (5'-CTC ACA ACC ATC TGT ATC TCA C-3'). The difference in size of the resulting PCR fragments reflects largely the loxP site with some additional sequence from the multi cloning site of vector pBS64. The *Jak2* null/knockout allele can

be detected by PCR after Cre mediated recombination of the floxed allele using the primers #1786 (5'-GTC TAT ACA CCA CCA CTC CTG-3') and #1787 (5'-GAG CTG GAA AGA TAG GTC AGC-3'). The expected PCR fragment for the knockout allele is about 400 bp in size.

Heterozygous floxed mice (*Jak2*$^{fl/wt}$) were mated to obtain mice with two copies of the floxed allele on the homologous chromosomes (*Jak2*$^{fl/fl}$) (Fig. 15). Homozygous mutant mice that carry two floxed *Jak2* alleles developed normally until adulthood. Both males and females were fertile, and they exhibited no obvious phenotypic abnormalities. Therefore, the insertion of the selectable marker upstream of the first coding exon had no effect on the transcriptional regulation of *Jak2*, and the floxed allele was phenotypically indistinguishable from its wild type counterpart. The statistical distribution of the mutant allele was according to Mendelian ratio. Therefore in contrast to conventional Jak2 knockout mice (5), embryonic lethality among our homozygous Jak2 conditional mutants was not observed.

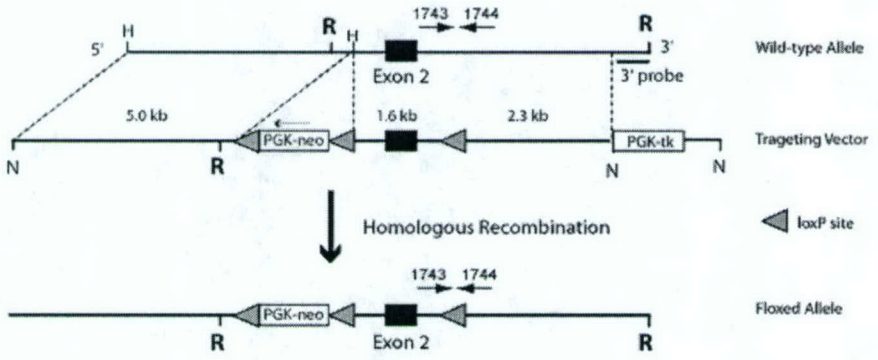

Figure 3: Targeting strategy to generate a conditional knockout allele for Jak2. A 3' probe (P) that is not part of the targeting vector was used to verify the targeting event. The primer pair 1743/1744 was used to verify the presents of the 3' prime loxP site and to distinguish the targeted floxed allele from the wild type *Jak2* locus by PCR.

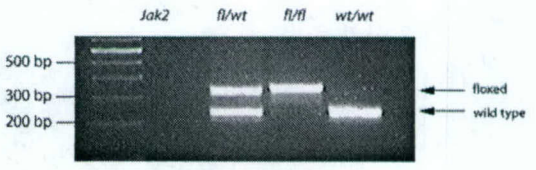

Figure 4: Genotyping results of mice using genomic DNA of tail biopsies and PCR with the primer pair 1743/1744. The difference in size of the resulting PCR fragments reflects largely the loxP site with some additional sequence from the multi cloning site of vector pBS64. Note that *Jak2*$^{fl/fl}$ mice do no show a PCR band for the wild type allele, and this result confirms a correct targeting event on the *Jak2* locus.

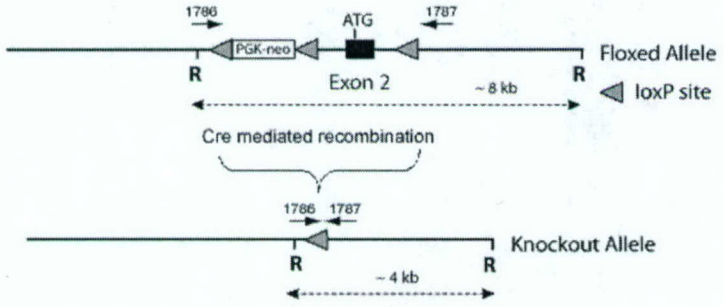

Figure 5. A conditional knockout of Jak2 is produced by Cre-mediated recombination deleting the first coding exon (exon 2) of Jak2. The excision of the exon can be confirmed by PCR (primer pair 1786/1787) and by Southern blot (8kb vs. 4kb) using *Eco*RI restriction digests.

Efficacy of the Cre-lox system as a potential technology to delete the *Jak2* locus in the mammary gland of genetically engineered mice: We have generated all the necessary tools and technologies that will allow us to conditionally delete the Jak2 gene in mammary epithelial cells *in vitro* and *in vivo*.

A. Gene deletion in vivo. A mammary-specific gene deletion can be achieved in adult mice using the **WAP-Cre** and **MMTV-Cre** transgenic lines, which we have published previously (6-8). All of our transgenic lines have already past the litmus test. With the help of these Cre mice, we have bypassed embryonic lethality that is otherwise associated with a ubiquitous inactivation of many genes. For instance, our Cre expressing mice have contributed to the generation of tissue-specific gene deletion models such as *Brca1* (9), *Bcl-x* (10), *PPARγ* (11), *Pten* (12), and *Tsg101* conditional knockouts (8). These mice, which are now being distributed by the Jackson Laboratory and the NCI Mouse Model Collective, are currently being used by many more investigators around the world.

There are differences in the Cre expression profile between WAP-Cre and MMTV-Cre transgenic mice that can be taken advantage of for in vivo targeting. Specifcally, ***WAP-Cre mice*** express their transgene almost exclusively in developing alveoli (luminal but *not* myoepithelial cells) during pregnancy and lactation, but not in ductal cells. ***MMTV-Cre mice*** express in epithelial cells of the ducts (luminal *and* myoepithelial cells) and developing alveoli. For the studies proposed in this grant, we will focus on deletion of the Jak2 gene from established mouse tumors using an in vitro approach.

Finally, to further restrict the activity of the recombinase to specific time points, we have generated a new retroviral vector (named pBabe-CrePR2) that expresses a ligand-inducible Cre enzyme. Cre was fused to the mutated ligand-binding domain of the progesterone receptor, which is able to bind RU486 but not progesterone (13).

D. STATEMENT OF THE WORK AND RESEARCH DESIGN

Specific Target #1: Establish whether Stat5 stimulates human breast cancer cell differentiation and adhesion, and suppresses tumor cell invasion, in vitro and in vivo.

Our overriding ***working hypothesis*** is that Stat5 maintains homotypic adhesion of a majority of human breast cancer cells by preserving normal E-cadherin/β-catenin complex, and inhibits the invasive characteristics of tumor cells.

Experimental Design: In order to test the working hypothesis, Stat5 activity has been experimentally manipulated in human breast cancer cells for *in vitro* studies of invasion and *in vivo* studies of peritumoral stromal invasion and metastasis in nude mice using a series of molecular tools that we have generated. These tools include **i)** Determine the invasion-related effects of Stat5-DN or Stat5-WT, with or without parallel Jak2-WT overexpression, by adenoviral gene delivery into established xenotransplants of human breast tumors *in vivo* in nude mice. *The parameters of invasion* that we have focused on are 1) homotypic cell adhesion, 2) cell motility, 3) peritumoral stromal invasion, and 4) metastasis and disease recurrence after surgical removal of xenotransplanted tumors.

Study #1. Adenoviral gene delivery - In vitro effect of Stat5 on homotypic adhesion, cell motility, and invasion. Adenoviral delivery is an effective vehicle for gene delivery into human epithelial cancer cells, which has the advantage over generating stable cell lines of allowing simultaneous

delivery of more than one gene product by viral co-infection. The invasion characteristics of the three human breast cancer cell types selected for study, ER (+) epithelioid lines of relatively weak metastatic potential, T47D, ZR75-1, and ER (-) epithelioid lines of relatively high metastatic potential, BT-20, overexpressing a Stat5-DN mutant or Stat5-WT, will be compared with cells infected with empty control adenovirus. The general adenoviral gene delivery scheme of T47D, ZR75-1, and BT-20, was as follows: a) Empty vector control; b) Stat5-DN; c) Stat5-WT; d) Stat5-DN+Jak2-WT; e) Stat5-WT + Jak2-WT; f) Jak2-DN; g) Jak2-WT. Viral infectivity parameters of human breast cancer cell lines T47D, ZR75-1, and BT-20 have been established. We have achieved 95-100% gene expression efficiency at a multiplicity of infection (MOI) of 10-25 for T47D and ZR75-1 cells, and at MOI of 25-40 for BT-20. We therefore anticipate using these viral doses for Stat5 suppression studies *in vitro*. Our experimental data have established that basal Stat5 activation and E-cadherin expression are present in T47D and ZR75-1 cells cultured in FCS, less detectable in BT-20.

After infection, cells were cultured and systematically compared with respect to homotypic cell adhesion, cell motility, *in vitro* invasion. Homotypic cell adhesion was analyzed by 1) cadherin immunocytochemistry and surface protein-biotinylation and detection (E-cadherin, N-cadherin, P-cadherin), and 2) immunohistochemistry and immunoblotting of catenins (β-catenin). Cell motility and invasion assay were been analyzed by Matrigel-based Boyden chamber assay.

Study #2. Stable gene introduction into human breast cancer cell lines - In vivo effect of Stat5 on homotypic adhesion, cell motility, and invasion. Human breast cancer cell lines T47D and MDA231 have be stably transfected with plasmids encoding Stat5-DN and Stat5-WT under tetracycline regulation (Tet-off) and the invasion-related regulatory effects of Stat5-DN or Stat5-WT will be tested. The inducible vector contains, in addition to the inserted Stat5 genes, both the neomycin resistance gene and the Tet-off regulated promoter. Thus, selectable and inducible gene expression will be achieved with a single plasmid in the absence of tetracyclin.

Expected Results of the study #2: The most important outcomes of these studies will be novel data mechanistically addressing the role of Stat5 in regulating E-cadherin/catenin complex, invasion, and metastatic potential in human breast cancer cells *in vitro* and in nude mice *in vivo*. These studies are important because new insight into the control of human breast cancer progression and metastasis will result.

Specific Target #2: Determine the effect of activated Stat5 on invasion and metastasis of mouse breast cancer models in vivo. This part has not been completed yet and is still undergoing investigation, Future work.

General Idea what this part of the research will be focused on:

The main question that will be addressed here is whether Stat5 stimulates homotypic breast cancer cell adhesion and inhibits metastatic invasion of mouse breast cancer models.

One important rationale for using murine breast cancer to model human breast cancer progression and invasion, centers on an important technical limitation of xenotransplants of human breast cancer in mice. Interactions between murine host peptide hormones/growth factors with receptor orthologs on human cancer cells are compromised due to evolutionary divergence between

species. For instance, murine prolactin and growth hormone do not activate the human ortholog receptors. It is therefore uncertain how biologically representative human cancer cells behave when placed in a murine mammary stroma within a murine endocrine environment.

We have carefully selected the murine mammary cancer model for the proposed studies that fulfills all of these criteria:

1) Tumors should be induced independent of Stat5 and its upstream activators, the Jak2 tyrosine kinase and prolactin receptors.
2) Tumors should be pregnancy-independent and be inducible in virgin mice.
3) Tumors should be ductal adenocarcinoma.
4) The tumor models should progress to metastasis with some frequency.
5) Stat5 should remain active in a significant portion of premetastatic tumors.

We will use the chemical carcinogenesis model of dimethyl-benz-anthracene (DMBA)-induced breast tumors, which gives rise to ductal adenocarcinomas at a median frequency of 37% in virgin mice without need for hormonal treatment, and metastasize to lung (14). Importantly, DMBA tumor model give rise to malignant tumors that maintain an active Stat5 pathway in well-differentiated adenocarcinomas. This model is therefore expected to be useful for testing the effect of inactivating Stat5 on tumor differentiation, invasion, and metastasis. An estimated number of thirty mice are needed to guarantee establishment of ten adenocarcinomas from each tumor model.

We will use two alternative strategies to inactivate Stat5 signaling in murine breast tumors:

1) ***Genetic deletion of the Stat5 tyrosine kinase, Jak2.***

To effectively inactivate Stat5 in established mouse tumors, our collaborator , Dr Wagner, has developed a novel conditional Jak2 knockout mouse model at the Eppley Cancer Center (15). This achievement uniquely effectively inactivates Stat5 by completely eliminating the Stat5 tyrosine kinase, Jak2, from mouse mammary tumor cells. It should be noted that no conditional gene knockout model exist that allows simultaneous elimination of the two highly homologous Stat5 genes, Stat5a and Stat5b.

2) ***Transient suppression of Stat5 activation***

To test whether transient suppression of Stat5 function in established tumors will cause increased invasion and metastasis, transplanted tumors also will be exposed to adenoviral delivery of DN-Stat5.

Expected Results:

We expect to have determined that loss Stat5 activation will cause breast tumor cell dedifferentiation and increase the ability of tumor cells to invade into peritumoral stroma and cause distant metastases. This expectation is based on our extensive preliminary data, and would support the novel concept of Stat5 as a gatekeeper of breast cancer invasion and metastasis. This is important

because these studies may lead to new therapeutic strategies to prevent and treat breast cancer metastases.

E. SOME HIGHLIGHTED RESULTS

Fig. 6. Activation of Stat5 is associated with increased E-cadherin levels in human T-47D breast cancer xenotransplants in vivo. To determine whether PRL-induced Stat5 activation would lead to elevated of E-cadherin levels in established T-47D xenotransplant tumors in nude mice, we injected tumor-bearing mice once daily with PRL for up to four days. Stat5 was not active in T-47D tumors when grown in nude mice as revealed by immunohistochemistry of active Stat5 in paraffin-embedded, formalin-fixed tumors, despite exposure to normal circulating levels of mouse PRL (Fig. 6, panel a). However, in response to injected human PRL Stat5 became activated as detected by nuclear localization of tyrosine phosphorylated Stat5 in tumors of PRL-treated animals at day 2 and 4 (Fig. 6, panels a). We then analyzed E-cadherin levels in the tumors by immunohistochemistry and immunocytochemistry.

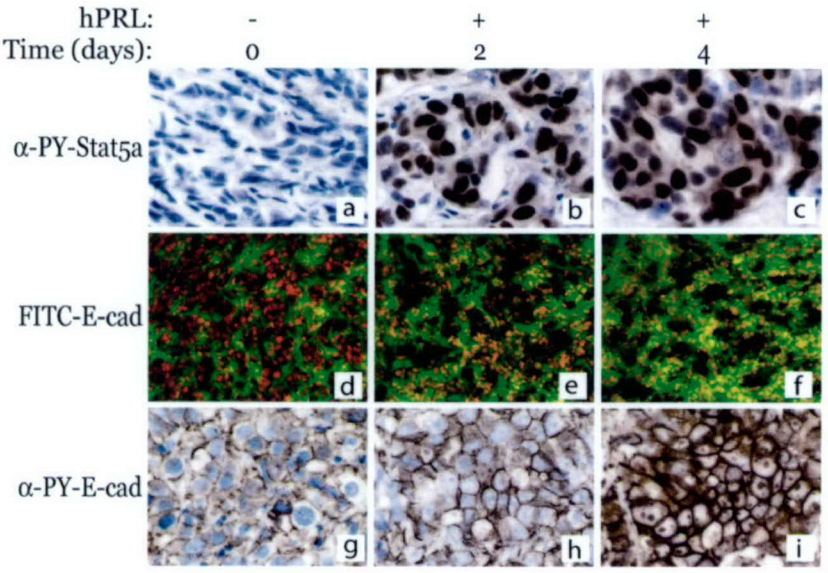

Immunostaining for E-cadherin on frozen sections and on sections of formalin-fixed, paraffin-embedded tumor tissues revealed that E-cadherin levels were low in untreated tumors, but were readily upregulated at the cellular junctions after 2 and 4 days of PRL treatment (Fig. 6, panels d-i). We conclude that treatment of nude mice carrying T-47D tumors with PRL led to activation of Stat5 in the tumors and increased levels of the homotypic adhesion molecule E-cadherin (16).

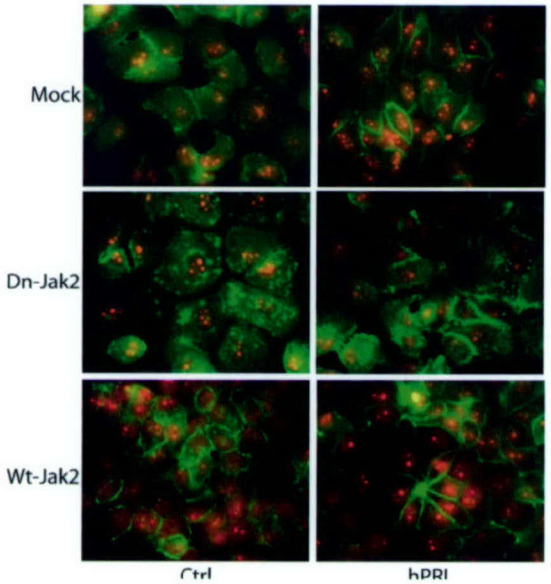

Fig. 7. PRL-induced upregulation of surface E-cadherin in T-47D cells requires the Stat5 tyrosine kinase, Jak2. The tyrosine kinase Jak2 is generally considered the mediator of PRL-induced tyrosine phosphorylation and activation of Stat5 in breast epithelia. We therefore predicted that blocking Jak2 activation would disrupt PRL-induced upregulation of E-cadherin at cellular junctions in T-47D cells. For these studies, T-47D cells were exposed to control virus or adenovirus carrying either dominant-negative Dn-*Jak2* or Wt-*Jak2*, and treated with or without PRL for 18 h. PRL enhanced E-cadherin staining intensity (Fig. 7, panels a, b) and this effect was blocked by Dn-Jak2 (Fig. 7, panels c, d), indicating that PRL enhancement of E-cadherin depended on Jak2 activation. Consistent with this notion,

overexpression of Wt-Jak2, which becomes autoactivated at elevated cellular concentrations, was associated with elevated E-cadherin levels in T-47D cells even in the absence of PRL, and did not block PRL-induced E-cadherin (Fig. 7, panels e, f). Taken together, our data demonstrated that the Stat5 tyrosine kinase, Jak2, is critical for PRL induction of E-cadherin in T-47D cells (16).

Fig. 8. Activation of Stat5a is associated with reduced invasion and migration of T-47D and BT-20 human breast cancer cell lines. The effect of PRL-activated Stat5a on invasive potential of T-47D and BT-20 breast cancer cells was next assessed *in vitro* by invasion and mobility assays. The ability of T-47D and BT-20 cells to invade through Matrigel-coated porous filters in response to a chemotactic stimulus was examined in a 8μm pore size Boyden chamber assay. Similarly, we tested the ability T-47D and BT-20 cells to migrate through uncoated porous filters. Invasion of T-47D and BT-20 through Matrigel-coated filters was modulated by Stat5 activation. Specifically, T-47D cell invasion was inhibited approximately 38% by PRL treatment, an effect that was blocked by adenoviral overexpression of Dn-Stat5 (Fig. 8 b, c, d,). Furthermore, overexpression of Wt-Stat5a was associated with highly reduced invasion in both untreated and PRL-treated T-47D cells, with as much as 67% inhibition when compared to mock-infected control cells (Fig. 8 e, f). In parallel experiments, BT-20 cells showed high basal invasion through Matrigel, and PRL alone did not inhibit invasion unless Wt-Stat5a was introduced into the cells (Fig. 8 g, h). Dn-Stat5 did not further enhance invasion of BT-20 cells through Matrigel (Fig. 8 i, j) (16).

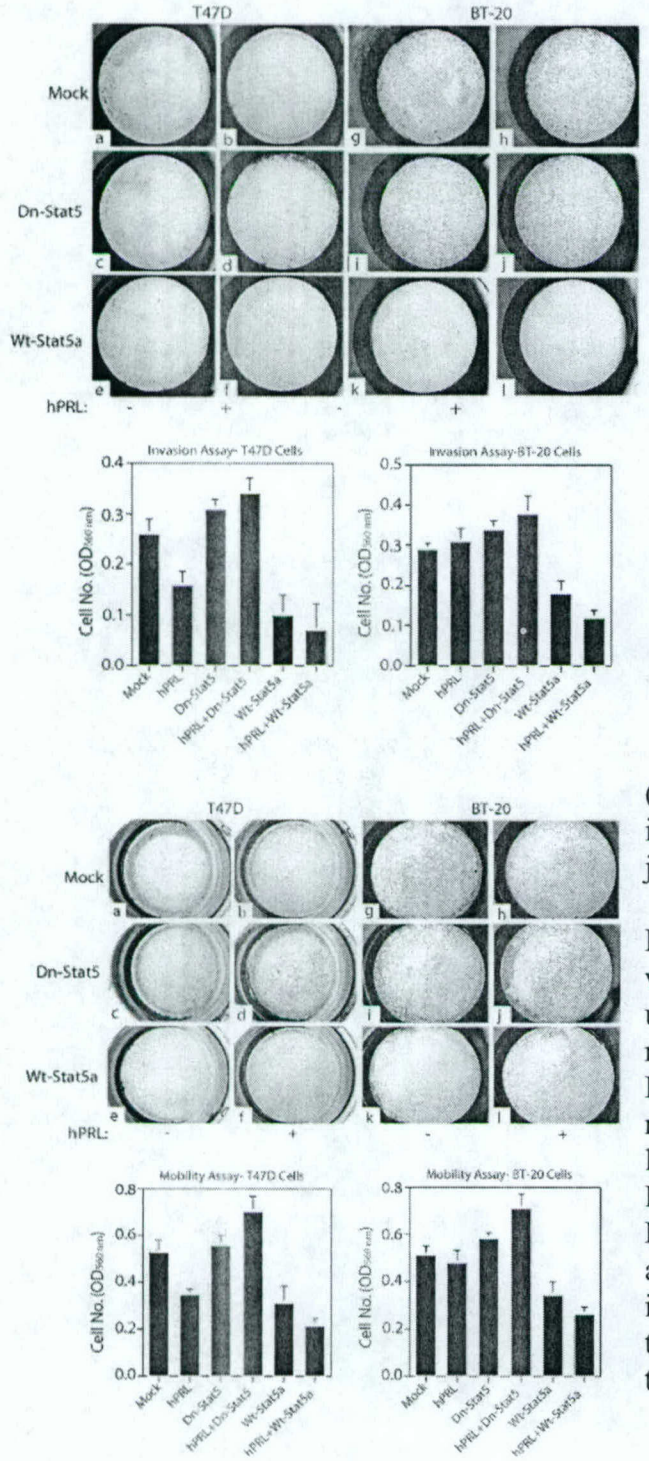

Fig. 9. Correspondingly, similar effects of Stat5 were detected in the migration assay through uncoated filters. T-47D cell migration was moderately inhibited by approximately 37% by PRL (Fig. 9 b). This PRL-induced inhibition was reversed by adenoviral delivery of DN-Stat5 to levels that were almost 2-fold higher than that of PRL-treated control cells (Fig. 9 c, d). Furthermore, overexpression of Wt-Stat5a was associated with an approximately 41% and 63% inhibition of migration in untreated and PRL-treated T-47D cells, respectively, when compared to mock-treated cells (Fig. 9 e, f). Parallel

experiments on BT-20 cells revealed that PRL alone did not inhibit migration, but that Dn-Stat5 in the presence of PRL moderately elevated the migration of BT-20 cells through the filters (Fig. 9 h, i, j). Furthermore, overexpression of Wt-Stat5a in the absence, and presence of PRL was associated with approximately 35-48% inhibition (Fig. 9 k, l). Collectively, the observations on cell invasion and migration of T-47D and BT-20 cells were highly consistent with the effects on homotypic adhesion and cell clustering, and provided further evidence that Stat5a inhibits the invasive phenotype of breast cancer cells (16).

F. KEY RESEARCH ACCOMPLISHMENTS

Summary of Progress and Significance of Data: In conclusion, our project supports the following notions:

a) Experimental inhibition of Stat5 signaling inhibits homotypic cell adhesion through the E-cadherin / β-catenin system, and stimulates invasion breast cancer cells *in vitro*.
b) Breast cancer progression is associated with loss of the Stat5 signaling.
c) We have generated a battery of molecular tools for experimental testing of the role of Stat5 in breast cancer invasion and metastasis, which is useful for mechanistically testing Stat5 role in breast cancer, including
1- Adenovirus Wt- and Dn- for Stat5 and Jak2.
2- A novel mouse model for conditional knockout of the Stat5 tyrosine kinase, Jak2.

G. REPORTABLE OUTCOMES:

Abstract presentation:
1- 5th Annual Lombardi Cancer Center Research, Georgetown University Medical Center, Washington DC, February 2004

2- 95th Annual Meeting, American Association of Cancer Research, AACR, Orlando, Florida, 27-31, 2004.

Manuscripts:

Sultan et al., Stat5 Promotes Homotypic Adhesion and Inhibits Invasive Characteristics of Human Breast Cancer Cells. Oncogene 2004, in press.

H. CONCLUSION:

The final conclusion of this work is summarized as the following:

First, our ***central hypothesis*** is Stat5 maintains homotypic adhesion of a majority of human breast cancer cells by preserving normal E-cadherin/β-catenin complexes, and inhibits the invasive characteristics of tumor cells.Stat5 activity has been experimentally manipulated in human breast cancer cells for *in vitro* studies of invasion and *in vivo* studies of peritumoral stromal invasion and metastasis in nude mice using a series of molecular tools that we have generated. These tools include viral and non-viral delivery of: a) wild-type (Wt) and dominant-negative (Dn) mutants of Stat5, b) Wt and Dn mutants of the Stat5 tyrosine kinase, Jak2, and c) antisense methodology for proven, effective suppression of Jak2.Stat5 activation acts as a invasive suppressor in breast cancer cells. This aspect

of the work is important because it could lead to new preventative and therapeutic strategies for primary and metastatic breast cancer.

Second, Loss of Stat5 activation (Stat5-pTyr) in primary human breast cancer is associated increased risk of latent, residual breast cancer and death in patients with lymph node-negative breast cancer. For that sake, Stat5 activation status in breast cancer is a useful clinical predictor of breast cancer progression and clinical outcome in lymph node-negative breast cancer. This is important because active Stat5 may serve as a simple immunohistochemical marker to distinguish node-negative breast cancer patients with excellent prognosis from patients with less favorable prognosis. Specifically, while patients at low risk may be spared for toxic and costly adjuvant therapies, others may require more aggressive therapy.

I. REFERENCES:

1- **Apantaku LM** 2000 Breast cancer diagnosis and screening. Am Fam Physician 62:596-602, 605-6

2-2002 WHO Statistical Information System. World Health Statistics Annual, World Health Organisation (WHO) Databank, Geneva, Switzerland, vol 2002.

3- **Xie J, LeBaron MJ, Nevalainen MT, Rui H** 2002 Role of tyrosine kinase Jak2 in prolactin-induced differentiation and growth of mammary epithelial cells. J Biol Chem 277:14020-30.

4- **Wagner KU, Claudio E, Rucker EB, 3rd, Riedlinger G, Broussard C, Schwartzberg PL, Siebenlist U, Hennighausen L** 2000 Conditional deletion of the Bcl-x gene from erythroid cells results in hemolytic anemia and profound splenomegaly. Development 127:4949-58.

5- **Neubauer H, Cumano A, Muller M, Wu H, Huffstadt U, Pfeffer K** 1998 Jak2 deficiency defines an essential developmental checkpoint in definitive hematopoiesis. Cell 93:397-409.

6- **Wagner KU, Wall RJ, St-Onge L, Gruss P, Wynshaw-Boris A, Garrett L, Li M, Furth PA, Hennighausen L** 1997 Cre-mediated gene deletion in the mammary gland. Nucleic Acids Res 25:4323-30.

7-**Wagner KU, McAllister K, Ward T, Davis B, Wiseman R, Hennighausen L** 2001 Spatial and temporal expression of the Cre gene under the control of the MMTV-LTR in different lines of transgenic mice. Transgenic Res 10:545-53.

8-**Wagner KU, Boulanger CA, Henry MD, Sgagias M, Hennighausen L, Smith GH** 2002 An adjunct mammary epithelial cell population in parous females: its role in functional adaptation and tissue renewal. Development 129:1377-86.

9- **Xu X, Wagner KU, Larson D, Weaver Z, Li C, Ried T, Hennighausen L, Wynshaw-Boris A, Deng CX** 1999 Conditional mutation of Brca1 in mammary epithelial cells results in blunted ductal morphogenesis and tumour formation. Nat Genet 22:37-43.

10- **Rucker EB, 3rd, Dierisseau P, Wagner KU, Garrett L, Wynshaw-Boris A, Flaws JA, Hennighausen L** 2000 Bcl-x and Bax regulate mouse primordial germ cell survival and apoptosis during embryogenesis. Mol Endocrinol 14:1038-52.

11- **Cui Y, Miyoshi K, Claudio E, Siebenlist UK, Gonzalez FJ, Flaws J, Wagner KU, Hennighausen L** 2002 Loss of the peroxisome proliferation-activated receptor gamma

(PPARgamma) does not affect mammary development and propensity for tumor formation but leads to reduced fertility. J Biol Chem 277:17830-5.

12- **Li G, Robinson GW, Lesche R, Martinez-Diaz H, Jiang Z, Rozengurt N, Wagner KU, Wu DC, Lane TF, Liu X, Hennighausen L, Wu H** 2002 Conditional loss of PTEN leads to precocious development and neoplasia in the mammary gland. Development 129:4159-70.

13- **Burcin MM, Schiedner G, Kochanek S, Tsai SY, O'Malley BW** 1999 Adenovirus-mediated regulable target gene expression in vivo. Proc Natl Acad Sci U S A 96:355-60.

14- **Wellbrock C, Geissinger E, Gomez A, Fischer P, Friedrich K, Schartl M** 1998 Signalling by the oncogenic receptor tyrosine kinase Xmrk leads to activation of STAT5 in Xiphophorus melanoma. Oncogene 16:3047-56.

15- **Bromberg JF, Wrzeszczynska MH, Devgan G, Zhao Y, Pestell RG, Albanese C, Darnell JE, Jr.** 1999 Stat3 as an oncogene [published erratum appears in Cell 1999 Oct 15;99(2):239]. Cell 98:295-303.

16- **Ahmed S. Sultan, Jianwu Xie, Matthew J. LeBaron, Erica L. Ealley, Marja T. Nevalainen, Hallgeir Rui.** Stat5 Promotes Homotypic Adhesion and Inhibits Invasive Characteristics of Human Breast Cancer Cells. Sultan et al., Oncogene 2004, in press.

ABSTRACT

Activation of Transcription Factor Stat5, but not Stat3, Inhibits Invasive Characteristics of Human Breast Cancer Cell lines

Ahmed S Sultan, Jianwu Xie, Jianqiong Zhu, Matthew J. LeBaron, and Hallgeir Rui
Georgetown University Medical Center, Lombardi Cancer Center, Washington DC, USA

Signal transducer and activator of transcription-5 (Stat5) is critical for breast epithelial cell differentiation and normal mammary gland development, especially the Stat5a gene product. Stat5a was originally described as a regulator of milk protein gene expression and subsequently shown to be essential for mammary development and lactogenesis. The role of Stat5 in invasion and metastasis of breast cancer cells has not been investigated. To examine whether activated Stat5 affects invasive characteristics of breast cancer cells, adenoviral gene delivery of wild type and dominant-negative (DN) mutants was used in a panel of human breast cancer cell lines. The cell lines analyzed, T47D, MCF-7, MDA-MB-231, MDA-MB-435, and BT-20, display different phenotypic characteristics ranging from poorly invasive to highly invasive. In the estrogen receptor (ER)-positive cell lines, T47D and MCF-7, which show high degree of Stat5 phosphorylation, sustained activation of Stat5, but not Stat3, led to formation of large cell clusters on Matrigel, and decreased cellular invasion two-fold in a Matrigel membrane invasion assay. Both cell cluster formation and reduced invasion were completely reversed by DN-Stat5, but not by DN-Stat3. In ER-negative cell lines, MDA-MB-231, MDA-MB-435, and BT-20, which show little or no Stat5 phosphorylation, adenoviral gene delivery of wild type Stat5 led to down-regulation of f-actin-based cell motility and decreased the formation of external hairy filopodia. In contrast, DN-Stat5 up-regulated f-actin-based cell motility, external filopodium formation and cellular invasion through a Matrigel membrane. Taken together, our data indicate that sustained activated Stat5, but not Stat3, inhibits invasive characteristics of breast cancer cells, and may shed new light on Stat5 involvement in breast cancer as an invasion suppressor.

Oncogene (2004) 00, 1–15

www.nature.com/onc

ORIGINAL PAPER

Stat5 promotes homotypic adhesion and inhibits invasive characteristics of human breast cancer cells

Ahmed S Sultan[1], Jianwu Xie[1], Matthew J LeBaron[1], Erica L Ealley[1], Marja T Nevalainen[1] and Hallgeir Rui*[,1]

[1]*Department of Oncology, Lombardi Comprehensive Cancer Center, Georgetown University Medical Center, NRB E504, 3970 Reservoir Rd NW, Washington, DC 20057-1469, USA*

Signal transducer and activator of transcription-5 (Stat5) mediates prolactin (PRL)-induced differentiation and growth of breast epithelial cells. We have recently identified active Stat5 as a tumor marker of favorable prognosis in human breast cancer, and determined that Stat5 activation is lost during metastatic progression. Here we provide novel evidence for an invasion-suppressive role of Stat5 in human breast cancer. Activation of Stat5 by PRL in human breast cancer lines was associated with increased surface levels of the invasion-suppressive adhesion molecule E-cadherin *in vitro* and in xenotransplant tumors *in vivo*. Inducible E-cadherin was blocked by dominant-negative (Dn) Stat5 or Dn-Jak2, but not by Dn-Stat3. Further experimental data indicated a role of Stat5 as a coordinate regulator of additional invasion-related characteristics of human breast cancer cells, including cell surface association of β-catenin, homotypic cell clustering, invasion through Matrigel, cell migration, and matrix metalloproteinase activity. A role of Stat5 as a suppressor of breast cancer invasion and metastatic progression provides a biological mechanism to explain the favorable prognosis associated with active Stat5 in human breast cancer.

Oncogene (2004) **0,** 000–000. doi:10.1038/sj.onc.1208203

Keywords: Stat5; breast cancer; E-cadherin; invasion; adhesion; motility; metastasis

Introduction

Signal transducer and activator of transcription-5 (Stat5) was originally identified as a prolactin (PRL) activated mammary gland transcription factor (Wakao *et al.*, 1994). A highly homologous Stat5b gene was also identified and was found to be expressed in the mammary gland (Liu *et al.*, 1995). Stat5a and Stat5b are activated by phosphorylation of a conserved tyrosine residue, which in turn facilitates homo- or heterodimerization, nuclear translocation, and binding of Stat5 to specific DNA response elements (Gouilleux *et al.*, 1994). Genetic studies have revealed that Stat5a and Stat5b mediate PRL-induced mouse mammary gland development (Liu *et al.*, 1997; Udy *et al.*, 1997). Specifically, Stat5a and Stat5b control growth and differentiation of the secretory alveolar cell compartment during pregnancy and lactation. While lactation is suppressed relatively more by genetic loss of Stat5a than Stat5b, Stat5b is still capable of compensating for loss of Stat5a so that lactation is restored in Stat5a null mice after multiple pregnancies (Liu *et al.*, 1998; Nevalainen *et al.*, 2002). Thus, the highly homologous Stat5a and Stat5b both promote mammary gland differentiation and development, despite the existence of subtle and possibly important differences in their structure and regulation (Grimley *et al.*, 1999; Kabotyanski and Rosen, 2003).

Initial investigations have indicated a mammary tumor-promoting role of Stat5 in mice, which is consistent with the established mammary tumor-promoting role of PRL in rodents (Clevenger *et al.*, 2003). Mammary tumorigenesis was delayed when the Stat5a gene was deleted in transgenic mice with mammary-directed expression of transforming growth factor-α (TGFα) or SV40 large-T antigen (Humphreys and Hennighausen, 1999; Ren *et al.*, 2002). In addition, transgenic overexpression of a constitutively active Stat5–Jak2 chimeric protein in the mouse mammary gland was associated with increased predisposition for mammary tumors (Iavnilovitch *et al.*, 2002). A cellular survival role of Stat5 has been described in preneoplastic and malignant mouse mammary epithelia (Humphreys and Hennighausen, 1999; Miyoshi *et al.*, 2001; Ren *et al.*, 2002), providing a possible mechanism for how Stat5 may promote mammary tumorigenesis in mice.

In human breast cancer, on the other hand, we have recently reported a favorable prognosis in patients whose tumors display active Stat5 (Nevalainen *et al.*, 2004). Our observations were based on detection of nuclear-localized, tyrosine-phosphorylated Stat5 in tumors of two independent clinical materials totaling more than 1000 patients. Active Stat5 in tumors specifically predicted reduced risk of both disease recurrence and death from breast cancer, particularly in early-stage cancer before lymph node metastases were detectable.

*Correspondence: H Rui, E-mail: ruih@georgetown.edu
Received 17 May 2004; revised 30 August 2004; accepted 17 September 2004

Journal: ONC ☐ Disk used Despatch Date: 30/10/2004
Article : npg_onc_2004-0793 Pages: 1–15 OP: Raj Ed: Viji

This prognostic value of Stat5 was independent of age, tumor size, histological grade, Her2/neu, and estrogen/progesterone receptor status (Nevalainen *et al*., 2004). Importantly, using the same phospho-Stat5 immunohistochemistry method, we have reported constitutive basal activation of Stat5 in healthy, nonpregnant human breast epithelia (Nevalainen *et al*., 2002) and found that inactivation or loss of Stat5 in human breast cancer correlated with metastatic progression (Nevalainen *et al*., 2004). In parallel work, human breast cancer histological differentiation was positively correlated with nuclear levels of Stat5 protein (Cotarla *et al*., 2004), as well as with nuclear levels of tyrosine-phosphorylated Stat5 (Nevalainen and Rui, in preparation).

Based on the new data on Stat5 activation in normal and malignant human breast, we hypothesized that the central role of Stat5 as a normal breast epithelial differentiation factor is maintained in early breast cancer, and that the favorable prognosis associated with active Stat5 is a result of inhibition by Stat5 of metastatic dispersal of cells from the primary tumor. We now report novel evidence for an invasion-suppressive role of Stat5 in human breast cancer cells. From studies of well-differentiated, estrogen receptor (ER)-positive T-47D and ZR-75-1 cells, and poorly differentiated, ER-negative BT-20 cells, systematic activation or inactivation of Stat5 revealed a broad role of Stat5 as a stimulator of homotypic cell clustering and cell surface accumulation of E-cadherin and surface-associated β-catenin. Moreover, Stat5 suppressed invasive features such as cell scattering, matrix metalloproteinase (MMP) secretion, cell invasion through Matrigel, and cell migration. Collectively, the observations support a novel role of Stat5 as a suppressor of breast cancer cell dispersal and metastatic progression, and provide a biological link between Stat5 activation and favorable prognosis in human breast cancer.

Results

Activation of Stat5 is associated with increased stability of cell surface E-cadherin in human breast cancer cell lines in vitro

To detect cell surface E-cadherin, cell surface proteins were first biotinylated and E-cadherin was subsequently immunoprecipitated from cell lysates using anti-E-cadherin antibodies, followed by detection of 120 kDa biotinylated E-cadherin by streptavidin-conjugated horseradish peroxidase. In parallel, whole-cell E-cadherin levels were analysed by Western blotting with specific E-cadherin antibody. In human breast cancer cell lines T-47D and ZR-75-1, but not BT-20, treatment with 20 nM PRL led to a marked accumulation of E-cadherin on the cell surface within 12–24 h (Figure 1A). Based on three experiments, reblotting with E-cadherin antibodies indicated that the overall cellular protein levels of E-cadherin did not change markedly in either of the three cell lines under the *in vitro* conditions used. Furthermore, N-cadherin or P-cadherin was not detected in either cell line, except for P-cadherin expression in BT-20 cells (data not shown).

Importantly, the ability of PRL to elevate cell surface E-cadherin levels in the three cell lines correlated with the ability of PRL to activate Stat5. In parallel experiments, PRL-inducible phosphorylation of Stat5a and Stat5b was determined in cells treated with or without 20 nM PRL for 15 min and analysed by Western blotting of Stat5a or Stat5b immunoprecipitated from whole-cell lysates using a specific anti-phospho-Stat5a/b (Tyr694/9) antibody. These experiments demonstrated that in T-47D and ZR-75-1 cells PRL induced rapid tyrosine phosphorylation of both Stat5a and Stat5b, while in BT-20 cells no detectable activation of either Stat5a or Stat5b was observed (Figure 1B). Taken together, these data supported the notion that Stat5 activation was associated with enhanced levels of E-cadherin on the surface of breast cancer cells.

Activation of Stat5 is associated with increased E-cadherin levels in human T-47D breast cancer xenotransplants in vivo

To determine whether PRL-induced Stat5 activation would lead to elevated E-cadherin levels in established T-47D xenotransplant tumors in nude mice, we injected tumor-bearing mice once daily with PRL for up to 4 days. Stat5 was not active in T-47D tumors when grown in nude mice as revealed by immunohistochemistry of active Stat5 in paraffin-embedded, formalin-fixed tumors, despite exposure to normal circulating levels of mouse PRL (Figure 1C, panel a). However, in response to injected human PRL, Stat5 became activated as detected by nuclear localization of tyrosine-phosphorylated Stat5 in tumors of PRL-treated animals at days 2 and 4 (Figure 1C, panels b and c). We then analysed E-cadherin levels in the tumors by immunohistochemistry and immunoblotting.

Immunohistochemistry for E-cadherin on sections of formalin-fixed, paraffin-embedded tumor tissues revealed that E-cadherin levels were low in untreated tumors, but were readily upregulated at the cellular junctions after 2 and 4 days of PRL treatment (Figure 1C, panels d–f). Independently, we determined total levels of E-cadherin in tumor homogenates by Western blotting. Clarified homogenates from frozen tumors from three mice in each treatment group were separated by SDS–polyacrylamide gel electrophoresis (SDS–PAGE) (20 μg/lane) and immunoblotted with antibodies to either E-cadherin or β-actin. Little or no E-cadherin was detectable in untreated tumors, while there was a time-dependent increase in the levels of E-cadherin in the tumors during 4 days of PRL treatment (Figure 1D). In contrast, levels of β-actin remained constant. We conclude that treatment of nude mice carrying T-47D tumors with PRL led to activation of Stat5 in the tumors and increased levels of the homotypic adhesion molecule E-cadherin.

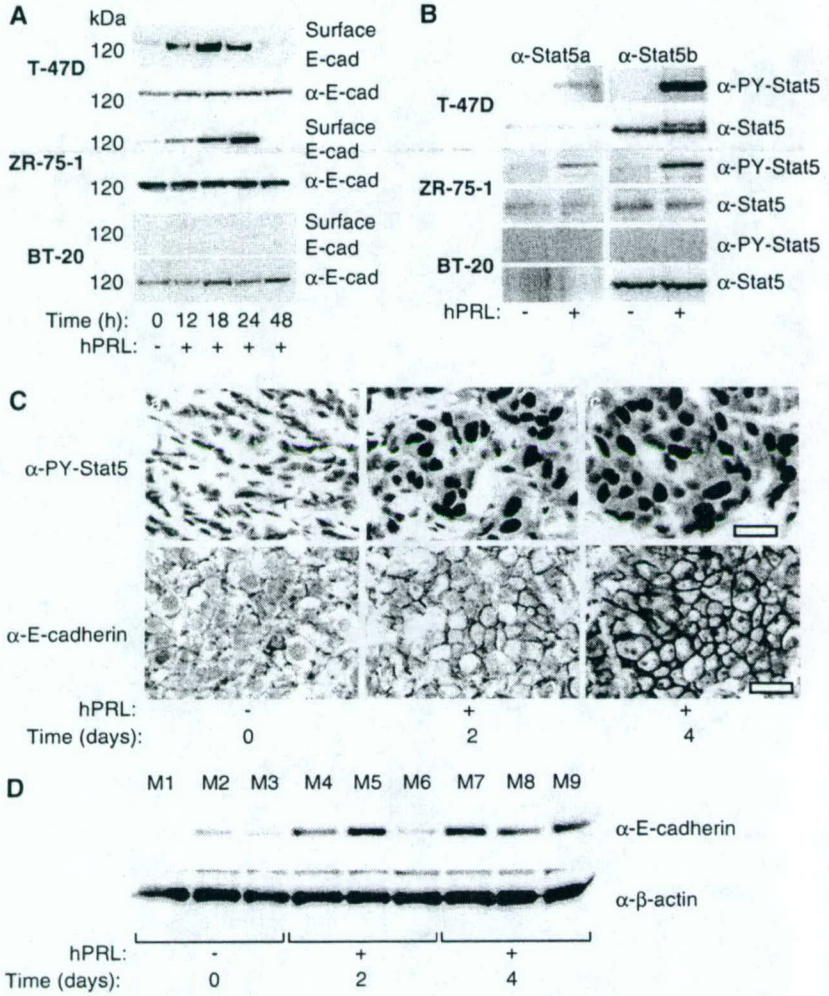

Figure 1 PRL-enhanced elevation of surface E-cadherin levels correlated with activation of Stat5 in human breast cancer cells *in vitro* and *in vivo*. (**A**) PRL enhancement of E-cadherin levels at cellular junctions. Levels of E-cadherin protein expressed on cell surface of T-47D, ZR-75-1, and BT-20 breast cancer cells were investigated after treatment with or without PRL for the indicated time intervals. Cell surface proteins were biotinylated and E-cadherin was immunoprecipitated from cell extracts, separated by 7% SDS–PAGE, and detected as a 120 kDa protein using streptavidin–horseradish peroxidase (upper panel). Total cellular levels of E-cadherin protein were analysed in parallel by Western blotting with specific antibodies to E-cadherin (lower panel). (**B**) PRL-induced Stat5 activation in breast cancer cell lines. Stat5a and Stat5b immunoprecipitated from whole-cell extracts of T-47D, ZR-75-1, and BT-20 breast cancer cells were examined for PRL-inducible tyrosine phosphorylation of Stat5a/b by anti-Stat5 pTyr antibodies (upper panel) or Stat5 protein levels (lower panel). (**C**) PRL-induced activation of Stat5 was associated with enhanced E-cadherin levels at cellular junctions in T-47D tumors *in vivo*. Human T-47D cells were grown as tumor xenotransplants in nude mice and mice were injected daily with saline or hPRL (5 μg/μg body weight, s.c.) for 0, 2, or 4 days. Sections of formalin-fixed, paraffin-embedded T-47D tumor xenotransplants were analysed by immunohistochemistry using a phosphospecific, anti-active Stat5 antibody (upper panel) or antibody to E-cadherin (lower panel), visualized and photographed using an Olympus Vanox Microscope equipped with a Zeiss $\times$ 40/0.8 NA objective lens (scale bar = 100 μm). (**D**) PRL stimulated E-cadherin protein levels in tumor xenotransplants *in vivo*. Total proteins extracted from tumors of nine mice (M1–M9), treated with PRL for 0, 2, or 4 days as indicated, were immunoblotted with antibodies to E-cadherin (upper panel) or β-actin to verify equal loading (lower panel). The *in vivo* experiments have been performed twice, and the *in vitro* experiments have been performed at least three times

Dn-Stat5, but not Dn-Stat3, disrupts PRL-induced E-cadherin stabilization on the surface of human T-47D breast cancer cells

Because we and others have reported that PRL activates other intracellular intermediaries in addition to Stat5 in T-47D cells, including Stat3 and the Ras–MAPK pathway (Erwin *et al*., 1995; Das and Vonderhaar, 1996; Schaber *et al*., 1998), we proceeded to test whether the mechanism of PRL-enhanced elevation of surface E-cadherin in T-47D cells required Stat5 activation. For these studies, we generated adenoviral gene vectors for high-efficiency delivery of dominant-negative (Dn) and wild type (Wt) Stat5a and Stat3. Because the C-terminal truncation mutant Stat5aΔ713 acts as a Dn for both Stat5a and Stat5b, we hereafter refer to this mutant as Dn-Stat5. T-47D breast cancer cells were incubated with

or without PRL for 18 h after gene delivery of either control vector, Dn-Stat5, or Wt-Stat5a. Parallel experiments correspondingly tested the effect of Dn-Stat3 or Wt-Stat3. PRL treatment enhanced E-cadherin levels at the cellular junctions as detected by immunofluorescence staining, leading to sharp distribution of green immunofluorescence at cell borders (Figure 2a and b, upper panels). Importantly, PRL-enhanced upregulation of surface E-cadherin was blocked by Dn-Stat5, but not by Dn-Stat3 (Figure 2a and b, middle panels). Consistent with a positive role of Stat5 in mediating PRL-enhanced upregulation of surface E-cadherin, overexpression of Wt-Stat5a enhanced PRL-induced elevation of surface E-cadherin levels (Figure 2a, lower panels). In contrast, Wt-Stat3 blocked PRL enhancement' effect on surface E-cadherin levels, leading to diffuse distribution of green immunofluorescence (Figure 2b, lower panels). We also verified the immunohistochemistry data by analysis of surface E-cadherin after cell surface biotinylation. Immunoblotting demonstrated that PRL-enhanced elevation of surface E-cadherin was effectively blocked by Dn-Stat5 (Figure 2c). Collectively, our data indicate that activation of Stat5, but not Stat3, mediates PRL-enhanced surface E-cadherin protein expression in T-47D breast cancer cells, and suggest that Stat3 may have an opposite effect compared to Stat5 on this parameter.

PRL stimulates cell surface accumulation of β-catenin in T-47D breast cancer cells

In epithelial cells, intracellular β-catenin typically associates with the cytoplasmic domain of E-cadherin when E-cadherin accumulates at the cell membrane. Upregulation of E-cadherin sequesters β-catenin from

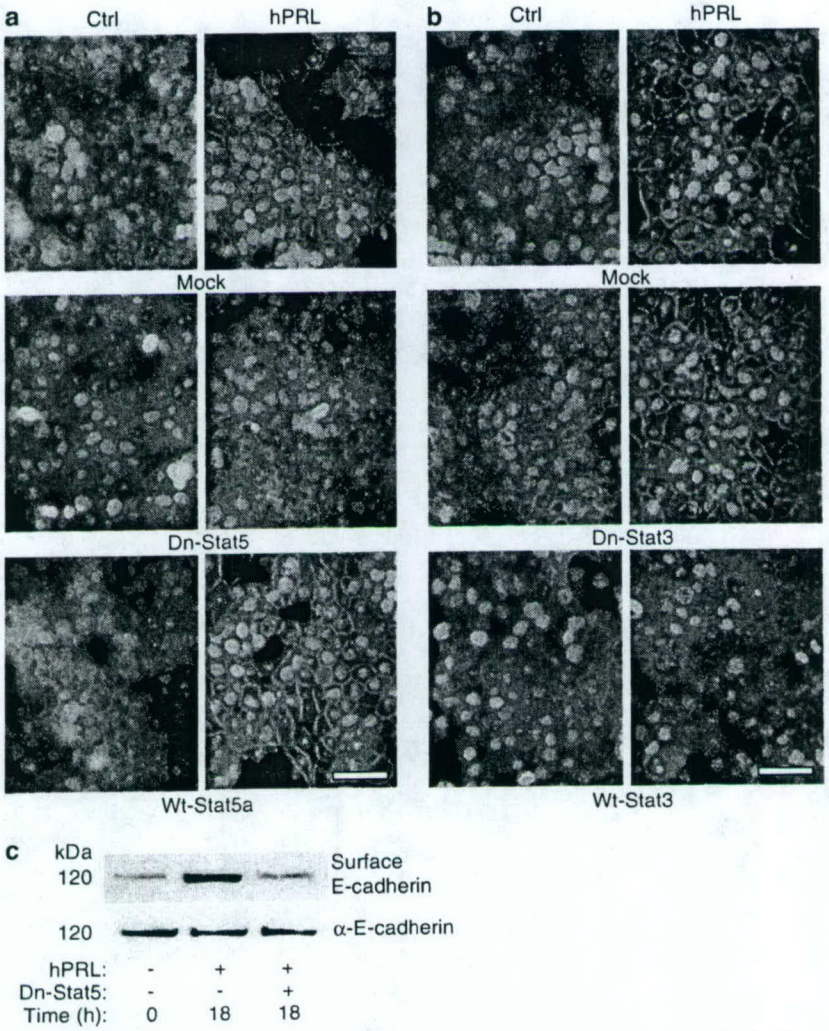

Figure 2 Dn-*Stat5*, but not Dn-*Stat3*, disrupted PRL-induced E-cadherin protein accumulation on cellular junctions in human T-47D breast cancer cells. Subconfluent T-47D cells were either mock infected or infected with adenovirus carrying Wt-*Stat5a* (**a**), Wt-*Stat3* (**b**), Dn-*Stat5* (**a**), or Dn-*Stat3* (**b**) at m.o.i. 25 for 90 min. After 16 h, T-47D cells were treated with or without PRL for 18 h, and cells were fixed, permeabilized, and stained for the presence of E-cadherin using FITC-conjugated secondary antibodies (green fluorescence). DNA was stained with propidium iodide (red fluorescence). Cells were visualized and photographed under fluorescence microscopy (original magnification, × 200; scale bar = 20 μm). Representative data from three independent experiments are shown

the cytoplasm and thereby prevents β-catenin from translocating to the nucleus where it may act as a transcriptional regulator (Stockinger *et al.*, 2001). The localization of β-catenin and E-cadherin as a complex at cell–cell adherens junctions is necessary for proper epithelial cell function and tissue integrity (Kemler and Ozawa, 1989), and this protein complex plays a key role in suppression of metastatic tumor progression (Mbalaviele *et al.*, 1996). To determine whether PRL-induced stabilization of E-cadherin on the cell surface of T-47D cells also was associated with β-catenin localization at the cell surface, cellular β-catenin localization was analysed by immunofluorescence staining. After exposing cells to control virus or adenovirus carrying either Dn-Stat5 or Wt-Stat5a, T-47D cells were treated with or without PRL for 18 h and cells were fixed and stained for the presence of β-catenin using FITC-conjugated secondary antibodies (green fluorescence). Similar to the surface localization of E-cadherin, PRL enhanced β-catenin accumulation at cell borders (Figure 3a, upper panel). PRL-induced accumulation of β-catenin at cellular junctions was blocked by Dn-Stat5, leading to diffuse distribution of green immunofluorescence and less marked staining at cell junctions (Figure 3a, middle panel). Furthermore, overexpression of Wt-Stat5a enhanced β-catenin localization to cell junctions, especially after activation by PRL (Figure 3a, lower panel).

PRL treatment of T-47D cells is associated with inhibition of EGF-induced tyrosine phosphorylation of β-catenin

Tyrosine phosphorylation of β-catenin has been reported to promote metastatic progression of tumor cells (Kinch *et al.*, 1995). Since EGF treatment is an established method for stimulating the tyrosine phosphorylation of β-catenin, T-47D cells were treated with 8 nM EGF for 30 min after activation of Stat5 by 20 nM PRL for different time intervals and were subjected to Western blot analysis. As shown in Figure 3b, there was a significant decrease in EGF-induced tyrosine phosphorylation of β-catenin at 18 h of PRL treatment, corresponding temporally with maximal enhancement of surface E-cadherin levels. Furthermore, EGF receptor autophosphorylation and expression levels remained constant throughout the experiment (Figure 3c). Taken together, Stat5 activation may not only enhance E-cadherin/β-catenin complex formation at cell–cell junctions in T-47D cells, but could also help stabilize the β-catenin protein by preventing its tyrosine phosphorylation.

PRL-enhanced upregulation of surface E-cadherin in T-47D cells requires the Stat5 tyrosine kinase Jak2

The tyrosine kinase Jak2 is generally considered as the mediator of PRL-induced tyrosine phosphorylation and activation of Stat5 in breast epithelia (Wagner *et al.*, 2004). We therefore predicted that blocking Jak2 activation would disrupt PRL-induced upregulation of E-cadherin at cellular junctions in T-47D cells. For these studies, T-47D cells were exposed to control virus or

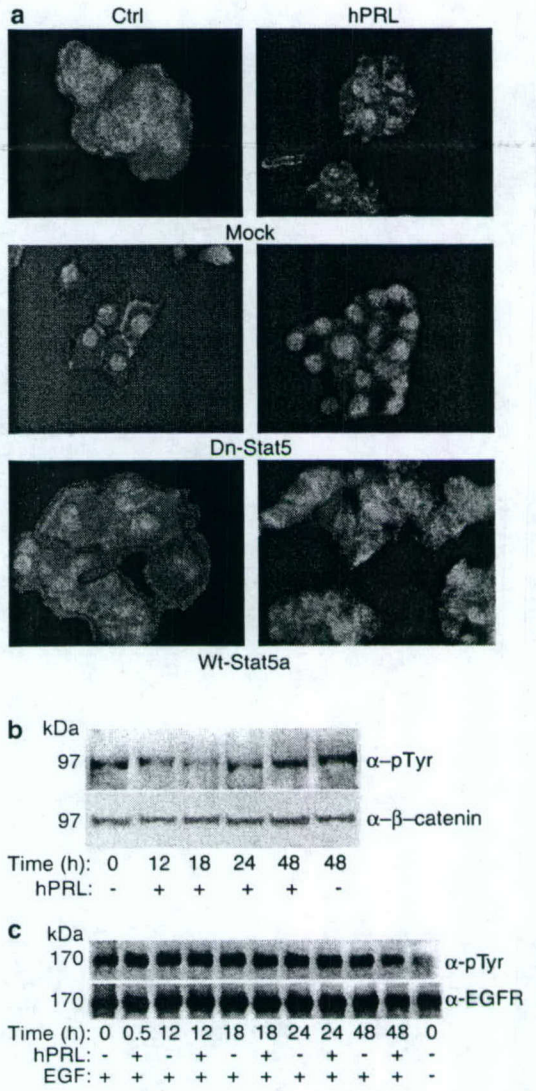

Figure 3 (**a**) Dn-Stat5 disrupted PRL-enhanced β-catenin localization at cellular junctions in T-47D breast cancer cells. Subconfluent T-47D cells were either mock infected or infected with adenovirus carrying Wt-*Stat5a* or Dn-*Stat5* at m.o.i. 25 for 90 min. After 16 h, T-47D cells were treated with or without PRL for 18 h and cell cultures were fixed, permeabilized, and stained for the presence of β-catenin using FITC-conjugated secondary antibodies (green fluorescence). DNA was stained with propidium iodide (red fluorescence). Cells were visualized and photographed under fluorescence microscopy (original magnification, × 400). (**b**) PRL-activated Stat5 inhibited EGF-induced tyrosine phosphorylation of β-catenin in T-47D breast cancer cells. T-47D cells incubated with PRL (20 nM) for the indicated times were collected after a brief exposure to EGF (8.0 nM) for 30 min. Immunoprecipitated (IP) β-catenin was separated by SDS–PAGE and analysed by anti-phosphotyrosine immunoblotting (upper panel). The membrane was reprobed with anti-β-catenin antibody to verify equal loading of precipitated proteins (lower panel). (**c**) EGF-R phosphorylation and protein levels in PRL-treated T-47D cells. Parallel cultures of T-47D cells were treated with or without PRL for the indicated time intervals and then stimulated with EGF (8.0 nM) for 30 min. EGF-R proteins were immunoprecipitated, resolved by 7% SDS–PAGE, and immunoblotted for tyrosine phosphorylation with anti-phosphotyrosine monoclonal antibody 4G10 (upper panel), and reprobed with anti-EGF-R (lower panel). Representative data from three independent experiments are shown

adenovirus carrying either Dn-*Jak2* or Wt-*Jak2* and treated with or without PRL for 18 h. PRL enhanced E-cadherin staining intensity at cell junctions (Figure 4a and b) and this effect was blocked by Dn-Jak2 (Figure 4c and d), indicating that PRL enhancement of E-cadherin depended on Jak2 activation. Consistent with this notion, overexpression of Wt-Jak2, which becomes autoactivated at elevated cellular concentrations, was associated with elevated E-cadherin levels in T-47D cells even in the absence of PRL and did not block PRL-induced E-cadherin (Figure 4e and f). Taken together, our data demonstrated that the Stat5 tyrosine kinase Jak2 is critical for PRL induction of E-cadherin in T-47D cells.

Stat5-dependent homotypic clustering of T-47D breast cancer cells on Matrigel

Reduced expression of E-cadherin in breast carcinomas is associated with increased risk of tumor invasion and metastasis as well as unfavorable prognosis (Berx and Van Roy, 2001). To investigate the role of Stat5 in the invasive capacity of human breast cancer cells, we examined the role of Stat5in homotypic cluster formation of T-47D cancer cells cultured on Matrigel, a collagen-rich extracellular matrix that provides a more physiological growth environment than plastic. T-47D cells cultured on Matrigel and treated with PRL showed significant morphological changes with formation of large cell clusters within 24 h as revealed by phase contrast stereomicroscopy (Figure 5a and b). PRL-induced cell clustering, as well as basal levels of cluster formation observed in control cells, was essentially eliminated in cells overexpressing Dn-Stat5, and the cells were instead highly scattered (Figure 5c and d). In contrast, overexpression of Wt-Stat5a markedly enhanced basal as well as PRL-induced cell clustering (Figure 5e and f). Based on these data, we conclude that activation of Stat5 induces aggregation of T-47D cells, consistent with increased homotypic adhesion and suggestive of reduced invasive potential.

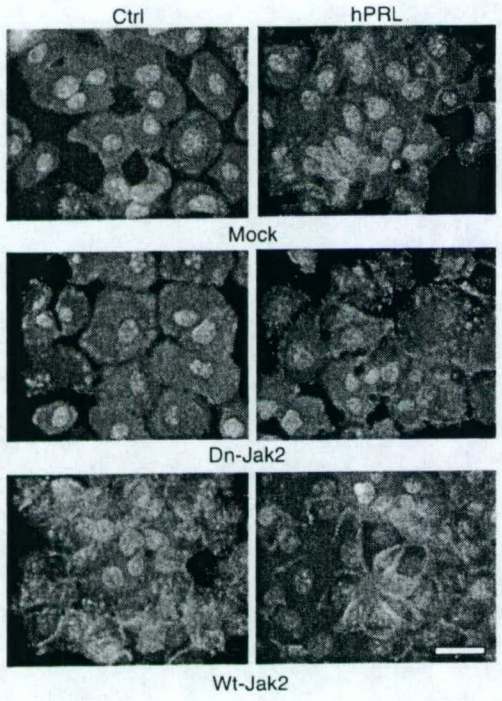

Figure 4 Targeted inhibition of the Stat5 tyrosine kinase Jak2 mimicked the disruptive effect of Dn-Stat5 on PRL-enhanced cell surface levels of E-cadherin in T-47D breast cancer cells. Subconfluent T-47D cells were either mock infected or infected with adenovirus carrying Wt-*Jak2* or Dn-*Jak2* at m.o.i. 10 for 90 min. After 16 h, T-47D cells were treated with or without hPRL for 18 h, fixed, permeabilized, and immunostained for the presence of surface E-cadherin using FITC-conjugated secondary antibodies. Cells were visualized and photographed under fluorescence microscopy (original magnification, × 400; scale bar = 20 μm). Representative images from one of three independent experiments are shown

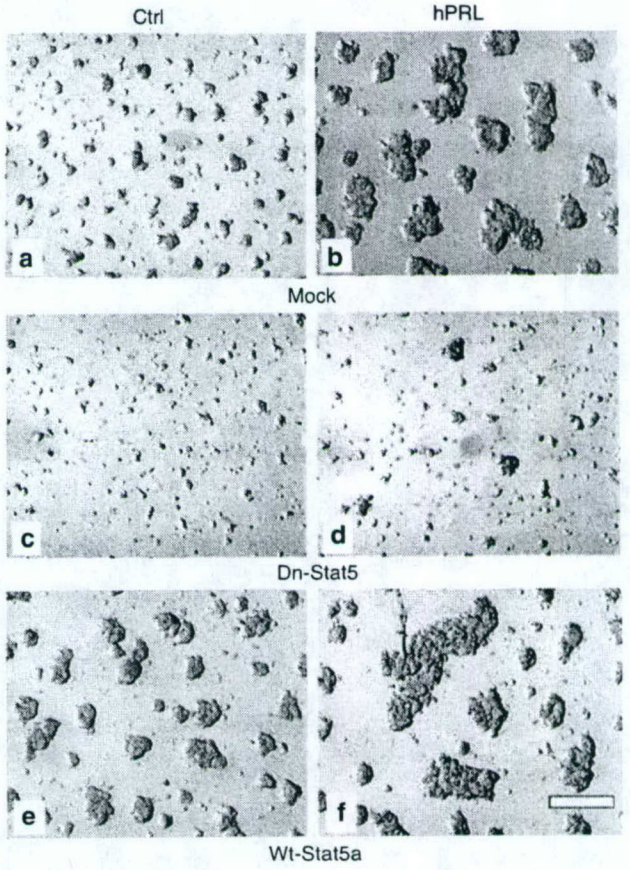

Figure 5 Dn-Stat5 disrupted PRL-induced homotypic cluster formation of T-47D breast cancer cells on Matrigel. T-47D cells seeded on Matrigel were either mock infected or infected with adenovirus carrying Wt-*Stat5a* or Dn-*Stat5a* at m.o.i. 25 for 90 min. After 16 h, T-47D cells were treated with or without PRL for 18 h and were fixed as described in Materials and methods. Morphological alterations of T-47D cells were visualized and photographed under phase contrast microscopy (Nikon Stereoscope) (scale bar = 300 μm). Representative images from one of three independent experiments are shown

Reconstitution of active Stat5a in BT-20 cells reverses undifferentiated, mesenchymal phenotype, and stimulates homotypic cell clustering on Matrigel

We then examined the effect of activation of Stat5 on homotypic cell clustering in BT-20 cells cultured on Matrigel. As previously shown (Figure 1), BT-20 cells, which are poorly differentiated and lack ERs, did not respond to PRL with Stat5 activation in contrast to more well-differentiated, ER-positive T-47D. Likewise, BT-20 cells showed little or no PRL-induced upregulation of surface E-cadherin in BT-20 cells (see Figure 1). Consistent with their mesenchymal or fibroblastoid phenotype, BT-20 cells did not form epithelioid clusters on Matrigel, and PRL alone could not overcome the natural scattering of BT-20 cells (Figure 6A, panels a and b). However, overexpression of Stat5a through adenoviral gene delivery led to robust clustering, which was moderately but consistently enhanced by PRL (Figure 6A, panels c and d). In contrast, overexpression of Dn-Stat5 did not induce cell clustering of BT-20 cells (Figure 6A, panels e and f). On the other hand,

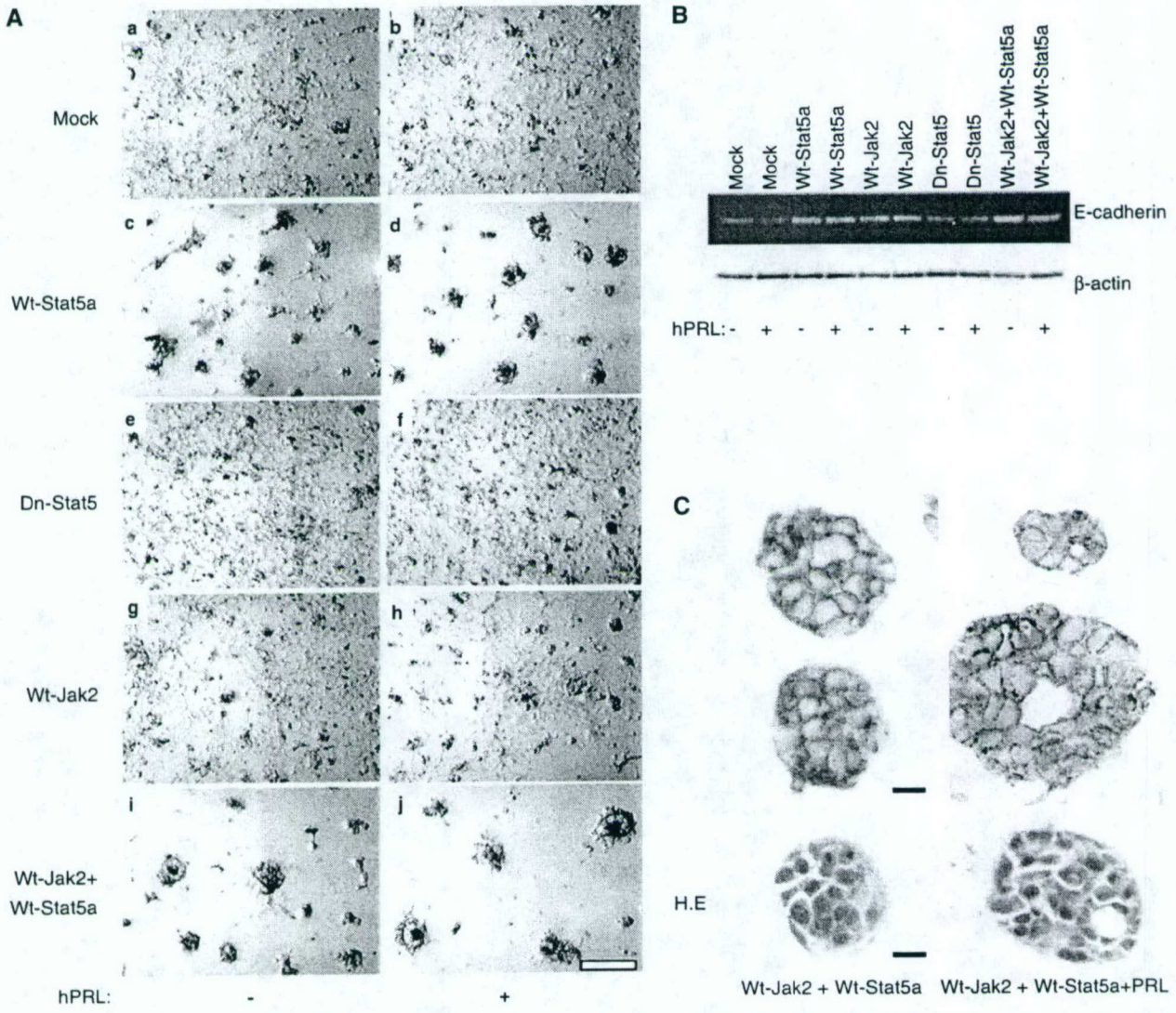

Figure 6 Reconstitution of activated Stat5 enhanced cell clustering and E-cadherin protein expression in BT-20 breast cancer cells on Matrigel. (**A**) BT-20 cells seeded on Matrigel were either mock infected or infected with adenovirus for 90 min as follows: Wt-*Stat5a* or Dn-*Stat5* at m.o.i. 25, Wt-*Jak2* at m.o.i. 5, or a combination of Wt-*Stat5a* at m.o.i. 25 plus Wt-*Jak2* at m.o.i. 5. After 16 h, BT-20 cells were treated with or without PRL for 3 days, and morphology was examined by stereomicroscopy (panels a–g; scale bar = 100 μm). (**B**) Enhanced E-cadherin levels in BT-20 cells after adenoviral delivery of Wt-Jak2 and Wt-Stat5. The change in the expression levels of E-cadherin was examined by Western blot SDS–PAGE from lysates of BT-20 cells treated in the same order as shown in (**A**). (**C**) E-cadherin localized at cell–cell borders in BT-20 cells. Sections of formalin-fixed, paraffin-embedded BT-20 cell spheroids induced by Jak2 and Stat5 were analysed for E-cadherin localization by immunohistochemical analysis. HE: hematoxylin and eosin staining of parallel sections. Cells were visualized and photographed using an Olympus Vanox Microscope equipped with a Zeiss × 40/0.8 NA objective lens (scale bar = 100 μm). Representative images from three independent experiments are shown

overexpression of Jak2 was associated with a modest but consistent induction of small cell clusters, especially in PRL-treated cells, an effect possibly mediated by activation of low levels of endogenous Stat5 (Figure 6A, panels g and h). Coexpression of both Wt-Stat5a and Wt-Jak2 markedly stimulated clustering of BT-20 cells on Matrigel (Figure 6A, panels i and j). The large clusters formed in response to Jak2 and Stat5 were reminiscent of alveolar-like structures, or mammospheres, that are induced by PRL–Jak2–Stat5 signaling in well-differentiated mammary epithelial cell lines such as Comma-D and HC-11 cells (Schmidhauser *et al*., 1992; Xie *et al*., 2002). This notion was supported by the appearance of collapsed domes in the fixed, dehydrated cell cultures (Figure 6A, panels i and j).

In parallel experiments using the same experimental conditions, we investigated whether inducible clustering of BT-20 cells on Matrigel was associated with increased cellular E-cadherin levels. Western blot analysis on whole-cell lysates showed elevated levels of E-cadherin under conditions where clustering occurred, with highest levels in BT-20 cells overexpressing Wt-Jak2 plus Wt-Stat5a, and lowest levels in control cells and cells expressing Dn-Stat5 (Figure 6B). In contrast, cellular β-actin levels remained unchanged. Immunohistochemistry of E-cadherin in sections of formalin-fixed, paraffin-embedded cellular clusters from Wt-Jak2 plus Wt-Stat5a-expressing cells revealed that E-cadherin was localized to the cellular junctions (Figure 6C, upper panels). While PRL treatment did not further elevate total E-cadherin levels, PRL-treated spheroids showed frequent evidence of central lumen formation and tended to be larger (Figure 6C, right panels). Based on these observations, we conclude that reconstitution of an activated Jak2–Stat5 pathway in poorly differentiated BT-20 breast cancer cells enhances E-cadherin levels, homotypic adhesion, and cell clustering.

Activation of Stat5a is associated with reduced invasion and migration of T-47D and BT-20 human breast cancer cell lines

The effect of PRL-activated Stat5a on the invasive potential of T-47D and BT-20 breast cancer cells was next assessed *in vitro* by invasion and mobility assays. The ability of T-47D and BT-20 cells to invade through Matrigel-coated porous filters in response to a chemotactic stimulus was examined in an 8 μm pore size Boyden chamber assay. Similarly, we tested the ability T-47D and BT-20 cells to migrate through uncoated porous filters. Invasion of T-47D and BT-20 through Matrigel-coated filters was modulated by Stat5 activation. Specifically, T-47D cell invasion was inhibited by approximately 38% by PRL treatment, an effect that was blocked by adenoviral overexpression of Dn-Stat5 (Figure 7b–d). Furthermore, overexpression of Wt-Stat5a was associated with highly reduced invasion in both untreated and PRL-treated T-47D cells, with as much as 67% inhibition when compared to mock-infected control cells (Figure 7e and f). In parallel experiments, BT-20 cells showed high basal invasion through Matrigel, and PRL alone did not inhibit invasion unless Wt-Stat5a was introduced into the cells (Figure 7g, h, k, and l). Dn-Stat5 did not further enhance invasion of BT-20 cells through Matrigel (Figure 7i and j).

Correspondingly, similar effects of Stat5 were detected in the migration assay through uncoated filters. T-47D cell migration was moderately inhibited by approximately 37% by PRL (Figure 8b). This PRL-induced inhibition was reversed by adenoviral delivery of Dn-Stat5 to levels that were almost twofold higher than that of PRL-treated control cells (Figure 8c and d). Furthermore, overexpression of Wt-Stat5a was associated with an approximately 41 and 63% inhibition of migration in untreated and PRL-treated T-47D cells, respectively, when compared to mock-treated cells (Figure 8e and f). Parallel experiments on BT-20 cells revealed that PRL alone did not inhibit migration, but that Dn-Stat5 in the presence of PRL moderately elevated the migration of BT-20 cells through the filters (Figure 8h–j). Furthermore, overexpression of Wt-Stat5a in the absence and presence of PRL was associated with approximately 35–48% inhibition (Figure 8k and l). Collectively, the observations on cell invasion and migration of T-47D and BT-20 cells were highly consistent with the effects on homotypic adhesion and cell clustering and provided further evidence that Stat5 inhibits the invasive phenotype of breast cancer cells.

Stat5a inhibits MMP activity in T-47D and BT-20 human breast cancer cell lines

We further examined whether the Stat5-dependent modulation of invasive features of T-47D and BT-20 cells also included levels of MMP activities that are associated with tumor invasiveness (Coussens and Werb, 1996). MMP activities were measured by a zymography assay in conditioned media from T-47D or BT-20 cells. Conditioned media from the well-differentiated T-47D cells showed no detectable MMP activities under basal or PRL-stimulated conditions. However, conditioned medium from T-47D cells following overexpression of Dn-Stat5 produced readily detectable gelatinolytic activity corresponding in size to MMP-2. This induction was enhanced by PRL treatment (Figure 9, upper panel). In contrast, T-47D cells overexpressing Wt-Stat5a displayed no basal or PRL-inducible MMP-2 activity (Figure 9, upper panel). In conditioned medium from poorly differentiated BT-20 cells, there were barely detectable gelatinolytic bands corresponding to MMP-9 independent of PRL treatment (Figure 9, lower panel). However, Wt-Stat5a overexpression in BT-20 cells was associated with reduction in the activity of MMP-9 in PRL-treated cells, whereas Dn-Stat5 overexpression slightly increased activity of MMP-9 (Figure 9, lower panel). Overall, the coordinated effects of Stat5 on MMP production in T-47D and BT-20 and other parameters of invasion, including invasion through Matrigel, motility, and homotypic adhesion, support the notion

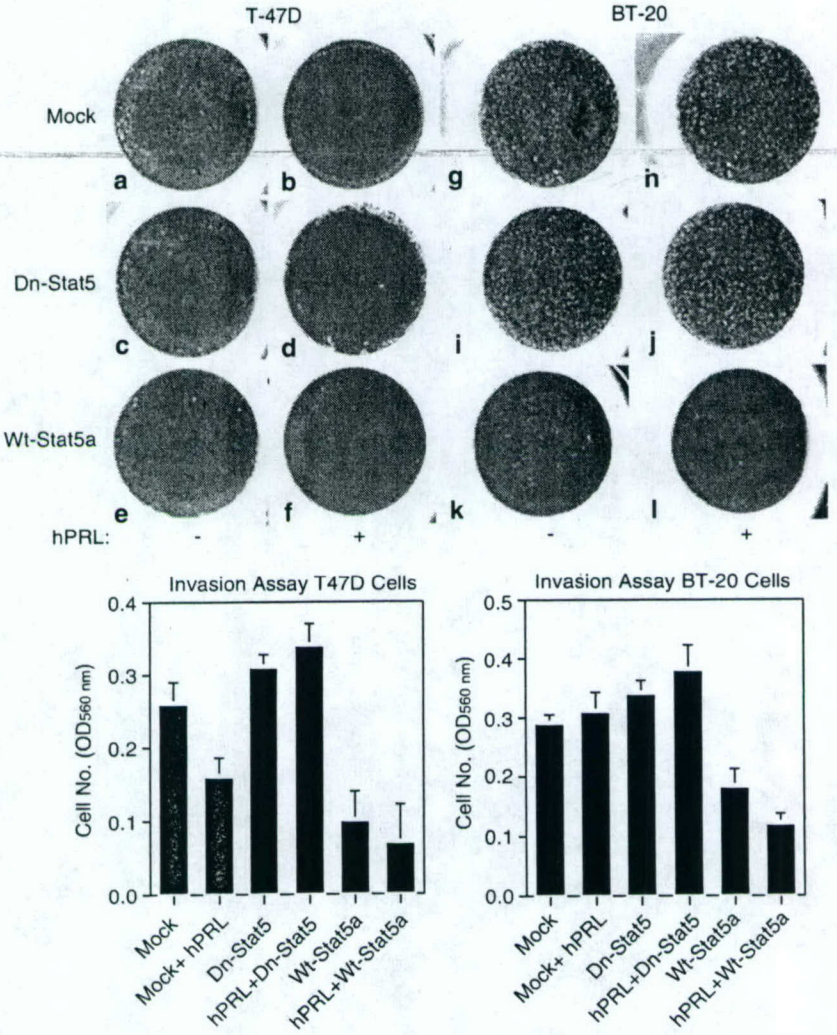

Figure 7 Activation of Stat5 inhibited invasion of T-47D and BT-20 breast cancer cells through Matrigel. T-47D or BT-20 cells were either mock infected or infected with adenovirus carrying Dn-*Stat5* or Wt-*Stat5a* at m.o.i. 25 for 90 min. Invasion through Matrigel-coated filters into the Transwell chambers of T-47D or BT-20 cells incubated in the presence or absence of PRL was measured 24 h later. The invading cells were stained as described in Materials and methods, and photographed using phase contrast microscopy (Nikon Stereoscope). Representative filters from individual experiments are shown. Invading cells were stained and quantified in triplicate filters in three individual experiments, and OD_{560} readings are presented (mean $\pm$ s.d.)

that Stat5 may suppress cellular invasion and metastasis *in vivo*.

Discussion

The present study provides novel evidence for a role of Stat5 as a suppressor of breast cancer cell invasion. Activation of Stat5 promoted homotypic adhesion of breast cancer cells, as evidenced by Stat5-mediated cell clustering and upregulation of cell surface E-cadherin and β-catenin. In parallel, Stat5 activation negatively regulated breast cancer cell invasion, migration, and MMP secretion. Importantly, combinatory gene delivery of the Jak2 tyrosine kinase and Stat5 into poorly differentiated, ER-negative BT-20 cells effectively restored homotypic cell adhesion and promoted cell clustering. The new data on Stat5 as a coordinate suppressor of invasive characteristics of human breast cancer cells provide a biological mechanism to explain our recent clinical observation that activation of Stat5 in human breast cancer is associated with favorable prognosis (Nevalainen *et al*., 2004).

We propose that Stat5 acts as a suppressor of invasion and dispersal of breast cancer cells from the primary tumor. This paradigm is novel in light of the breast tumor-promoting role that has been attributed to Stat5 (Humphreys and Hennighausen, 1999; Iavnilovitch *et al*., 2002; Yamashita *et al*., 2003), and also unexpected since Stat5 may facilitate mesenchymal transition in kidney epithelial cells (Benitah *et al*., 2003). However, an invasion-suppressive role of Stat5

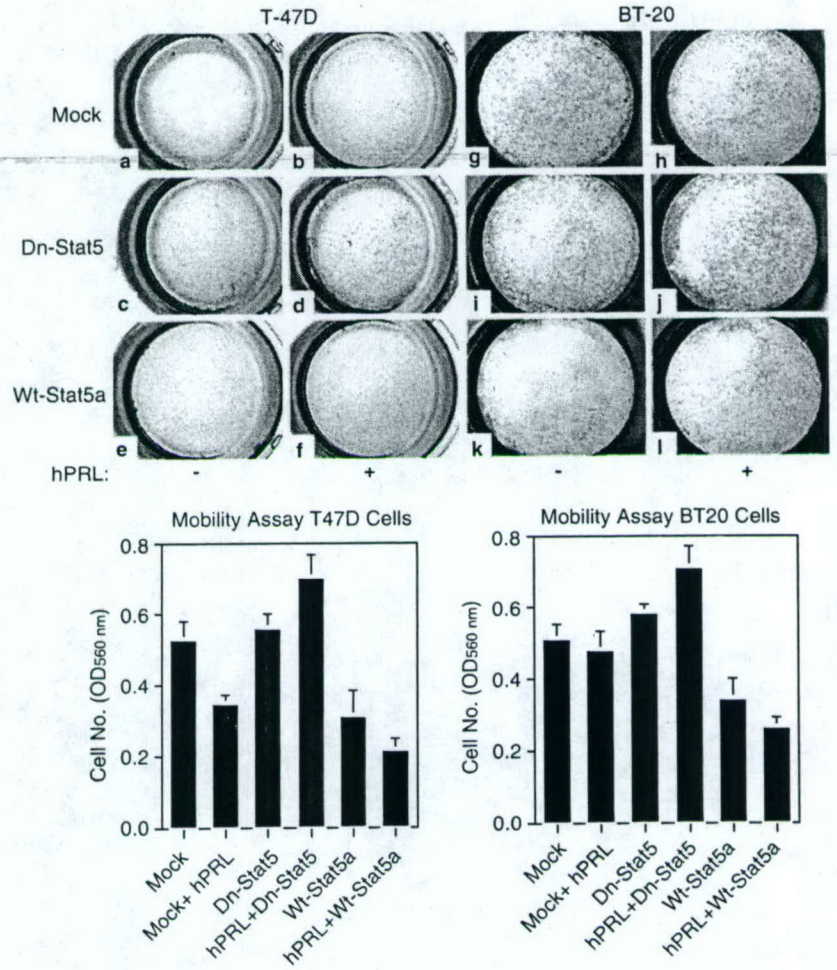

Figure 8 Activation of Stat5 inhibited cell motility of T-47D and BT-20 breast cancer cells. T-47D or BT-20 cells were exposed to mock infection or infection with adenovirus carrying either Dn-*Stat5* or Wt-*Stat5a* at m.o.i. 25 for 90 min. Motility through uncoated filters into the Transwell chambers of T-47D or BT-20 cells incubated with or without PRL was measured after 24 h. Migrating cells were fixed, stained, and photographed under phase contrast microscopy (Nikon Stereoscope). Representative filters from individual experiments are shown. Invading cells were stained and quantified in triplicate filters in three individual experiments, and OD_{560} readings are presented (mean ± s.d.)

is consistent with a series of other experimental observations in normal and malignant breast epithelial cells. First, the data presented in this report provide direct evidence for an invasion-suppressive role of Stat5 in human breast cancer lines. Second, Stat5 is a key regulator of epithelial differentiation in mouse mammary gland (Kazansky *et al*., 1995; Liu *et al*., 1996, 1997; Teglund *et al*., 1998), and Stat5 likewise is hyperactivated during terminal differentiation and lactation in human breast (Nevalainen *et al*., 2002). Third, in human breast cancer, activation of Stat5 correlated positively with histological differentiation (Cotarla *et al*., 2004). Finally, Stat5 is active in normal human breast epithelia and loss of basal Stat5 activation correlated with metastatic progression of human breast cancer (Nevalainen *et al*., 2004). Collectively, the data indicate that Stat5 maintains cellular differentiation, promotes homotypic adhesion, and inhibits cellular invasion of human breast cancer, and suggest that Stat5 activation in tumors could be causally linked to the markedly reduced risk of latent disease in patients with lymph node-negative breast cancer (Nevalainen *et al*., 2004).

The positive effect of Stat5 on homotypic breast cancer cell clustering was associated with enhanced accumulation of surface E-cadherin and β-catenin, key protein components of intercellular adherens junctions. Compelling evidence exists to indicate that downregulation of E-cadherin expression or function is a critical event in early metastatic progression of most epithelial tumors, including breast cancer (Bukholm *et al*., 1998; Fearon, 2003; Wheelock and Johnson, 2003). While E-cadherin protein levels increased in T-47D tumors in nude mice following 2–4 days of Stat5 activation, total cellular E-cadherin protein levels increased less than the marked increase in cell surface-exposed E-cadherin in

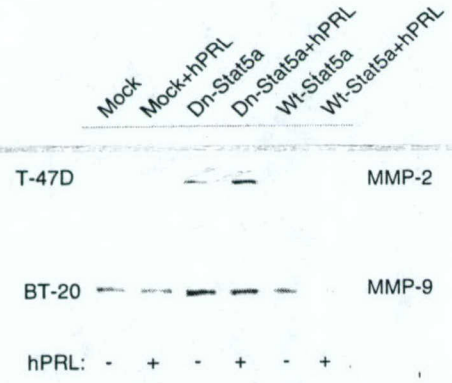

Figure 9 Activation of Wt-Stat5 and Dn-Stat5 modulated MMP levels in T-47D and BT-20 human breast cancer cell lines. T-47D or BT-20 cells were exposed to mock infection or adenovirus carrying either Dn-*Stat5* or Wt-*Stat5a* at m.o.i. 25 for 90 min. Samples of conditioned medium collected from T-47D or BT-20 cells treated with or without PRL for 30 h were analysed for gelatinolytic activity by gel zymography. Representative data from three independent experiments are shown

monolayer culture. The stimulatory effect of Stat5 on breast cancer E-cadherin levels therefore may not simply reflect a direct transcriptional induction of the E-cadherin gene. Increased stabilization of E-cadherin on the cell surface may in part be due to reduced rates of protein turnover (Le *et al*., 1999; Paterson *et al*., 2003). Furthermore, activation of Stat5 was associated with reduced EGF-induced tyrosine phosphorylation of β-catenin, and with enhanced localization of β-catenin at cell–cell contacts in T-47D cells. Increased tyrosine phosphorylation of β-catenin correlates with the disassembly of adherens junctions and decrease of cell–cell adhesion, and occurs during malignant transformation and tumor invasion (Behrens *et al*., 1996; Papkoff, 1997; Lilien *et al*., 2002). Stat5-induced adherens junction formation in breast cancer cells may therefore involve multiple molecular mechanisms.

The PRL-induced enhancement of surface E-cadherin levels detected in T47D cells was blocked by Dn-Stat5 but not by Dn-Stat3. Intriguingly, Wt-Stat3 also blocked PRL-induced enhancement of surface E-cadherin levels, suggesting that Stat5 and Stat3 exert opposing effects on adherens junction formation in breast cancer cells. Future studies will investigate the mechanisms by which Stat5 and Stat3 transcription factors may differentially affect surface E-cadherin levels. The observed opposite effect of Stat5 and Stat3 on cell adhesion may also be of relevance to mammary gland involution at the end of the lactation cycle, a process in which Stat5 maintains the secretory tissue architecture and cell survival, whereas Stat3 facilitates epithelial involution and massive apoptosis (Chapman *et al*., 1999; Groner and Hennighausen, 2000).

MMPs may contribute to metastatic dispersal of cancer cells by degrading extracellular matrix and facilitating intravasal growth (Kim *et al*., 1998). A very recent study reported that PRL may inhibit MMP expression in T-47D cells (Philips and McFadden, 2004), an observation that could be mediated through PRL-induced Stat5 activation, which is consistent with the present work on Stat5 as a suppressor of invasive characteristics. In contrast, two previous reports have suggested that PRL may increase invasiveness of T-47D cells based on *in vitro* studies. In one study, this interpretation was based on reduced adhesion of T-47D cells to the plastic growth support after extended PRL treatment for 6 days (Shiu and Paterson, 1984). However, this effect may be secondary to PRL-induced homotypic cell–cell adhesion, especially in light of the parallel evidence of PRL-induced differentiation of the T-47D cells in the same cultures. The second study used wound closure assay and a Boyden chamber setup that involved placement of PRL as a chemoattractant in the target compartment (Maus *et al*., 1999). The reported positive effects of PRL on T-47D cell migration may be mediated by PRL-induced signals other than Stat5 under the culture conditions used, which included exogenous insulin and hydrocortisone in the medium. For instance, Stat3, mitogen-activated protein kinases (MAPKs), c-Src, or focal adhesion kinase may also be activated by PRL in T-47D cells (Schaber *et al*., 1998; Acosta *et al*., 2003). Specifically, Stat3 and MAPK were found to be involved in interleukin-6-induced migration of breast cancer cells (Arihiro *et al*., 2000; Badache and Hynes, 2001). Furthermore, peptide growth factors and culture conditions may directly affect PRL signaling (Marte *et al*., 1995; Yamashita *et al*., 1999), and context-dependent PRL signaling may contribute to the complex roles of PRL in human breast cancer development and progression (Clevenger *et al*., 2003). Finally, in some experimental settings, and especially when T47D cells were exposed to Matrigel (e.g. Figures 5 and 7), Stat5 overexpression alone exerted some effect even in the absence of PRL, indicating that Stat5 is activated by other factors under these conditions.

In summary, the present study provides novel evidence for a role of Stat5 as a suppressor of human breast cancer invasiveness. This notion is consistent with the significantly reduced risk of disease recurrence in lymph node-negative breast cancer in which Stat5 is active (Nevalainen *et al*., 2004). Ongoing work will determine whether Stat5 directly inhibits metastasis formation of human breast cancer in athymic nude mice. Future studies will also identify the mechanisms underlying Stat5-induced upregulation of E-cadherin at cellular junctions in breast epithelial cells. Finally, the restoration of homotypic clustering of the ER-negative BT-20 breast cancer cell line by gene delivery of Jak2 and Stat5 may be explored as a new strategy for metastasis-suppressive differentiation therapy.

Materials and methods

Cell culture

Breast carcinoma cell lines T-47D, ZR-75-1, and BT-20 were obtained from American Type Culture Collection (ATCC, Manassas, VA, USA) and were maintained in Dulbecco's modified Eagle's medium (DMEM) containing 10% fetal

bovine serum (FBS; GIBCO, Carlsbad, CA, USA), 2 mM L-glutamine, and penicillin/streptomycin (Sigma, St Louis, MO, USA) (50 IU/ml) at 37°C with 5% CO_2. Unless stated otherwise, subconfluent cells in 75 cm^2 flasks were washed with phosphate-buffered saline (PBS) and maintained in DMEM with 2% FBS for 24 h before treatment with or without 20 nM human PRL for 18 h. Cell numbers were determined by a Beckman Coulter Counter (Fullerton, CA, USA).

Antibodies and reagents

Human PRL (NIDDK-PRL-SIAFP-B2, AFP-2969A) was kindly provided by Dr AF Parlow under the sponsorship of the National Hormone and Pituitary Program, National Institutes of Health (NIH) and the US Department of Agriculture. Mouse monoclonal antibodies against human E-cadherin (G10) and human β-catenin, and rabbit polyclonal antibody against human EGF-R were obtained from Santa Cruz Biotechnology (Santa Cruz, CA, USA). For immunohistochemistry of formalin-fixed, paraffin-embedded tissue, mouse anti-human E-cadherin antibody NCH-38 from Dako-Cytomation (Carpinteria, CA, USA) was used. Monoclonal anti-phosphotyrosine-Stat5 antibody (AX1) and polyclonal rabbit antisera to Stat5a (AX551) and Stat5b (AX554) were provided by Advantex BioReagents (Conroe, TX, USA), and monoclonal anti-phosphotyrosine antibody 4G10 was from Upstate Biotechnology (Lake Placid, NY, USA). A detection kit (Vectastain ABC) based on horseradish peroxidase–avidin complex and a fluorescent anti-mouse IgG kit were obtained from Vector Laboratories (Burlingame, CA, USA). Protein G–Sepharose 4FF beads and enhanced chemiluminescence (ECL) reagents were obtained from Amersham Pharmacia Biotech (Piscataway, NJ, USA). The bicinchoninic acid (BCA) kit for protein detection was obtained from Pierce (Rockford, IL, USA).

Generation of adenoviral vectors for high-efficiency gene delivery of Wt and Dn forms of Stat5, Stat3, and Jak2

Expression vector for murine Stat5a (pXM-Stat5a) was kindly provided by Xiuwen Liu and Lothar Hennighausen (NIH, Bethesda, MD, USA). A C-terminally truncated variant of Stat5a (Stat5aΔ713) that blocks both Stat5a and Stat5b-mediated gene transcription and was derived by deletion after amino-acid residue Ala-713 of pXM-Stat5a was subcloned, in parallel with the matching Wt-Stat5a cDNA, into the pShuttle-CMV transfer vector of the AdEasy adenoviral vector system (Qbiogene, Carlsbad, CA, USA) as described (Ahonen *et al*., 2003). To generate a parallel set of reagents for Stat3, full-length human Stat3 cDNA open reading frame was cloned from a human placenta cDNA library (J Xie and H Rui, unpublished data). Wt-Stat3 cDNA, and a Dn variant of Stat3 (Dn-Stat3Δ715) derived by truncation of the Wt-Stat3 cDNA by replacing the codon for amino-acid residue Thr-716 with a stop codon were used. Adenoviruses carrying Wt-Jak2 or a kinase domain deleted Dn-Jak2 with C-terminal V5/His epitope tags were derived from rat Jak2 constructs that we have previously described (Duhe *et al*., 1995; Xie *et al*., 2002) and were subcloned into the pShuttle-CMV transfer vector of the AdEasy system. In all cases, selected recombinant viral stocks were expanded in large-scale QBI-293A cells (Qbiogene, Carlsbad, CA, USA), purified by double cesium chloride gradient centrifugation, and titered using a standard plaque assay in QBI-293A cells.

Cell surface biotinylation

Cell surface biotinylation was performed as described previously with minor modifications (Sultan *et al*., 1997). Briefly, cells were grown to semiconfluence in 75 cm^2 dishes, washed three times with ice-cold PBS, and biotinylated with 0.5 mg/ml sulfo-NHS-LC-Biotin in PBS (Pierce, Rockford, IL, USA) for 30 min on ice. Excess reagent was quenched and removed by washing with ice-cold DMEM containing 10% FBS. Cells were then resuspended in 0.5 ml of the following lysis buffer (50 mM Tris, pH 7.4, 150 mM NaCl, 5 mM EDTA, 1% Triton X-100/1% deoxycholate) containing 1 mM phenylmethylsulfonyl fluoride and 10 μg/ml each of aprotinin, leupeptin, antipain, and pepstatin.

After centrifugation at 15 000 *g* for 20 min at 4°C, equal amounts of protein were immunoprecipitated with 5 μg/ml of monoclonal anti-E-cadherin antibody at 4°C overnight, followed by incubation with Protein G–Sepharose 4 FF beads for 1.5 h. Immunoprecipitates were washed five times in lysis buffer, solubilized in SDS electrophoresis sample buffer, separated on a 7% SDS gel, and transferred to a polyvinylidene fluoride membrane (Millipore, Bedford, MA, USA). After blocking the membranes with 3% (w/v) skim milk in Tris-buffered saline containing 0.1% (v/v) Tween 20 (TBST, pH 7.5), the biotinylated proteins were visualized using the Vectastain ABC kit. After five washes of 10 min each with PBS containing 0.05% Tween 20, the membranes were treated with ECL Western blotting detection reagents for 1 min at room temperature and were exposed to BioMax film (Eastman Kodak, Rochester, NY, USA).

Immunoprecipitation and immunoblotting

Monolayers of cells were washed with PBS at room temperature and extracted on ice with 2.5 ml/75 cm^2 flask of the following lysis buffer (10 mM Tris-HCl (pH 7.6), 5 mM EDTA, 150 mM NaCl, 30 mM sodium pyrophosphate, 50 mM sodium fluoride, 1 mM sodium orthovanadate, 1% Triton X-100, 1 mM phenylmethylsulfonyl fluoride, 5 μg/ml aprotinin, 1 μg/ml pepstatin A, 2 μg/ml leupeptin).

The cells were lysed and the insoluble material was removed by centrifugation at 15 000 *g* for 20 min at 4°C. For immunoprecipitation, 500 μg of protein lysate was incubated with antibody overnight at 4°C. Protein A–agarose for the polyclonal antibodies or Protein G–Sepharose 4 FF for the monoclonal antibodies was added for an additional 1 h at 4°C. Agarose pellets were washed three times in the above lysis buffer and bound proteins were removed by boiling in SDS electrophoresis sample buffer. Lysates or immunoprecipitates were separated on 4–12 or 7% SDS–PAGE as indicated and transferred electrophoretically to polyvinylidene fluoride membrane (Millipore, Bedford, MA, USA). For immunoblotting, blocking buffer was TBS-T (0.15 M NaCl, 0.1% Tween 20, 50 mM Tris, pH 8.0) with 3% bovine serum albumin (BSA). Secondary antibody was goat anti-mouse immunoglobulin conjugated to horseradish peroxidase and antibody binding was detected using ECL. When needed, blots were stripped in buffer (2% SDS, 0.1 M 2-mercaptoethanol, 62.5 mM Tris, pH 6.8) at 70°C for 80 min and rinsed extensively in TBS-T before being reprobed.

Analysis of E-cadherin levels in T-47D xenograft tumors in vivo

Ovariectomized female athymic nude mice ($N = 12$, 6–8 weeks of age) with s.c. implants of slow-release 17 β-estradiol pellets (1.7 mg, 30-day release; Innovative Research of America, Sarasota, FL, USA) were inoculated s.c. with human T-47D cells (5×10^6 cells suspended in 200 μl of 50% Matrigel (BD

Biosciences, Bedford, MA, USA) and 50% RPMI-1640 (Biofluids, Rockville, MD, USA) into each of two dorsolateral sites. After 14 days, the nine mice with most consistent paired tumors of approximately 4 mm^3 each were selected and randomly distributed into three groups. The mice were treated daily with PRL (s.c. 5 μg/g body weight; Nevalainen *et al.*, 2002) for 0, 2, or 4 days in the continued presence of estrogen implants. At 3 h after final injections, mice were euthanized and the two tumors were harvested from each mouse. Each tumor was split into two, and one-half was snap-frozen on dry ice for analysis of E-cadherin levels in tumor extracts or by immunohistochemistry of frozen sections, and the other half was fixed in 10% buffered formalin for paraffin embedding and immunohistochemical analysis of Stat5 activation or E-cadherin. Immunohistochemical detection of nuclear-localized, tyrosine-phosphorylated Stat5 was performed using monoclonal antibody AX1 as described previously (Nevalainen *et al.*, 2002). Immunohistochemical detection of E-cadherin was performed by diaminobenzidine-based staining of paraffin-embedded sections using monoclonal antibody (DakoCytomation). For bright field imaging, an Olympus Vanox Microscope equipped with a Zeiss $\times$ 25/0.8 NA objective lens was used. For fluorescence imaging, a Nikon Eclipse E600 fluorescence microscope was used. Proteins were extracted from frozen tumors by homogenization in T-PER reagent (Pierce) and were analysed by Western blotting using specific E-cadherin monoclonal antibody.

Immunofluorescence staining of E-cadherin and β-catenin

Immunofluorescence measurements were performed as described (Zhang *et al.*, 1999). Briefly, cells were grown to subconfluence on glass coverslips in six-well tissue plates and were either mock infected or infected with adenovirus carrying Wt-*Stat5a*, Wt-*Stat3*, Wt-*Jak2*, Dn-*Stat5*, Dn-*Stat3*, or Dn-*Jak2* as indicated for 90 min. For all adenoviral infections, multiplicity of infection (m.o.i.) 25 was used, except for Wt- and Dn-*Jak2* (m.o.i. 10). After 16 h, cells were treated with or without 20 nM PRL for 18 h. Adherent cells on coverslips were washed once with PBS (10 mM sodium phosphate, pH 7.4, 140 mM NaCl, 3 mM KCl), fixed in 4% paraformaldehyde in PBS for 15 min, and then permeabilized by 0.5% Triton X-100 in PBS for another 15 min. Nonspecific binding was prevented by incubation in PBS containing 5% BSA for 30 min. Cells were then incubated for 2 h with mouse monoclonal antibodies to E-cadherin or β-catenin, at a final concentration of 800 ng/ml in PBS containing 5% BSA. Coverslips were washed to remove unbound antibodies and further incubated for 30 min with FITC-conjugated goat anti-mouse secondary antibody (Vector Laboratories) and DNA was stained with propidium iodide. After final washing, coverslips were mounted using the Prolong antifade kit (Molecular Probes, Eugene, OR, USA) and cells were visualized and photographed under a Nikon Eclipse E600 fluorescence microscope at $\times$ 200 magnification for E-cadherin and $\times$ 400 magnification for β-catenin.

Tyrosine phosphorylation of β-catenin and EGF-R

T-47D cells were plated at a density of 4×10^4 cells in 75-cm^2 dishes and cultured in DMEM containing 10% FBS for 48 h. The resulting subconfluent cells were further cultured for 24 h in DMEM containing 2% FBS, treated with or without 20 nM PRL for up to 48 h as indicated. Immediately before collection, cells were exposed to 8.0 nM EGF for 30 min. After washing with ice-cold PBS, cells were lysed in lysis buffer for 30 min on ice and insoluble components were removed by centrifugation at 15 000 *g* for 20 min at 4°C. β-Catenin and EGF-R were immunoprecipitated using monoclonal anti-β-catenin antibody or polyclonal anti-EGF-R, respectively, subjected to 7% SDS–PAGE, and immunoblotted with anti-phosphotyrosine monoclonal antibody, 4G10. After stripping, the membranes were reblotted for β-catenin protein or EGF-R protein.

Analysis of homotypic clustering of breast cancer cells on Matrigel

T-47D or BT-20 cells were seeded on glass coverslips coated with 0.5 ml of Matrigel (10 mg/ml) in six-well plates for 48 h. Cells were either mock infected or infected with adenovirus carrying Wt-*Stat5a* or Dn-*Stat5* at m.o.i. 25 for 90 min. BT-20 cells were either mock infected or infected with adenovirus carrying Wt-*Jak2*, Wt-*Stat5a*, Dn-*Stat5*, or a combination of Wt-*Jak2* and Wt-*Stat5* at m.o.i. 25 for Wt-*Stat5* or *Dn-Stat5* and at m.o.i. 5 for Wt-*Jak2* for 90 min. The resulting subconfluent cultures were further incubated for 24 h in DMEM containing 2% FBS and were then treated with medium alone (control) or 20 nM PRL. After 24–72 h of incubation at 37°C, cells were fixed as indicated in 4% paraformaldehyde in PBS for 15 min. Cells were washed twice with PBS and cell morphological alterations were analysed using phase contrast microscopy (Nikon Stereoscope, Chuo-ku, Japan) at $\times$ 200 magnification. BT-20 cell clusters induced by Wt-*Jak2* plus Wt-*Stat5* were subjected to further analysis for E-cadherin localization by immunohistochemistry, using specific E-cadherin monoclonal antibody, visualized, and analysed under Vanox Microscope equipped with a Zeiss $\times$ 25/0.8 NA objective lens.

Assays of cell invasion and cell mobility

The ability of breast cancer cells to migrate (mobility) was analysed using a Boyden chamber (Transwell filters unit, pore size 8 μm; Becton Dickinson & Co., Bedford, MA, USA) according to standard protocols (Albini *et al.*, 1987). For the invasion assay, Transwell filter units were used that had been precoated with a barrier of extracellular matrix, Matrigel (50 μm). In both assays, fibroblast conditioned medium, which was obtained by a 24 h incubation of NIH-3T3 cells with 50 μg/ml ascorbic acid in serum-free DMEM, was placed in the lower chamber as a chemoattractant. Cells were either mock infected or infected with adenovirus carrying Wt-*Stat5a* or Dn-*Stat5* at m.o.i. 25 for 90 min and treated with or without 20 nM PRL for 18 h as described above. Single-cell suspensions were obtained by treatment with PBS containing 5 mM EDTA, washed, and placed at 10^5 cells per well into the upper chamber in 0.5 ml DMEM containing 0.1% BSA in the presence or absence of 20 nM PRL for 24 h. Cells that had not penetrated the filter were wiped out with cotton swabs, and cells that had migrated to the lower surface of the filter were stained with 0.5% crystal violet, photographed, and quantified by dissolving stained cells in 10% acetic acid and measuring optical density at 560 nm. The data represent the average of three independent experiments with the s.d. indicated.

Zymography for gelatinolytic activity

Secreted metalloproteinase (MMP) activities were detected and characterized by zymography as previously described (Yasumitsu *et al.*, 1992). Conditioned media were obtained after a 30 h incubation period of cells that had either been mock infected or infected with adenovirus carrying Wt-*Stat5a* or Dn-*Stat5* at m.o.i. 25 for 90 min and treated with or without 20 nM PRL during the 30 h period. No detectable change in cell number was observed during this brief treatment period. MMPs were extracted using Gelatin Sepharose 4B beads

(Amersham Pharmacia Biotech, Piscataway, NJ, USA) that had been washed three times with equilibration buffer, pH 7.5 (50 mM Tris, 150 mM NaCl, 5 mM $CaCl_2$, 0.02% Tween 20, 0.07% Brij 35, 10 mM EDTA). A 100 μl portion of equilibrated Gelatin Sepharose beads was added to 4 ml of conditioned medium and samples were placed on an end-over-end shaker overnight at 4°C to allow the binding of gelatinases to the Gelatin Sepharose. Nonspecific binding was removed by washing Gelatin Sepharose beads with the equilibration buffer containing 200 mM NaCl, and MMPs were eluted with 20 μl of nonreducing 2 × Tris-glycine-SDS sample buffer. Samples were subjected to a 10% polyacrylamide gel impregnated with gelatin (1 mg/ml). Electrophoresis was performed under nonreducing conditions at 125 V for 2 h at 4°C. After electrophoresis, gels were rinsed twice in 2.5% (w/v) Triton X-100 and three times in double-distilled H_2O at room temperature, incubated at 37°C for 48 h in enzyme buffer (50 nM Tris-HCl, pH 7.8, 5 mM $CaCl_2$, 0.15 M NaCl, 1% (w/v) Triton X-100) and, then stained with a solution containing 0.1% (w/v) Coomassie brilliant blue R-250, 12.5% (v/v) ethanol, and 7.5% (v/v) acetic acid. The gels were destained in 45% methanol and 10% acetic acid in H_2O. Gelatinolytic enzymes were detected as transparent bands after Coomassie blue staining.

Acknowledgements

This work was supported by Public Health Service Grants DK52013 and CA101841 (to HR) from the National Institutes of Health (NIH), and DAMD17-03-1-0616 (to ASS) from the US Department of Defense. We thank The Lombardi Comprehensive Cancer Center's shared resources of Microscopy and Imaging, Tissue Culture, and Histology (supported in part by NIH 1P30-CA-51008). We also thank Eva C Andersson for assistance with immunohistochemical analysis of E-cadherin in BT-20 cells.

Q7

References

Acosta JJ, Munoz RM, Gonzalez L, Subtil-Rodriguez A, Dominguez-Caceres MA, Garcia-Martinez JM, Calcabrini A, Lazaro-Trueba I and Martin-Perez J. (2003). *Mol. Endocrinol.*, **17,** 2268–2282.

Ahonen TJ, Xie J, LeBaron MJ, Zhu J, Nurmi M, Alanen K, Rui H and Nevalainen MT. (2003). *J. Biol. Chem.*, **278,** 27287–27292.

Albini A, Allavena G, Melchiori A, Giancotti F, Richter H, Comoglio PM, Parodi S, Martin GR and Tarone G. (1987). *J. Cell Biol.*, **105,** 1867–1872.

Arihiro K, Oda H, Kaneko M and Inai K. (2000). *Breast Cancer*, **7,** 221–230.

Badache A and Hynes NE. (2001). *Cancer Res.*, **61,** 383–391.

Behrens J, von Kries JP, Kuhl M, Bruhn L, Wedlich D, Grosschedl R and Birchmeier W. (1996). *Nature*, **382,** 638–642.

Benitah SA, Valeron PF, Rui H and Lacal JC. (2003). *Mol. Biol. Cell*, **14,** 40–53.

Berx G and Van Roy F. (2001). *Breast Cancer Res.*, **3,** 289–293.

Bukholm IK, Nesland JM, Karesen R, Jacobsen U and Borresen-Dale AL. (1998). *J. Pathol.*, **185,** 262–266.

Chapman RS, Lourenco PC, Tonner E, Flint DJ, Selbert S, Takeda K, Akira S, Clarke AR and Watson CJ. (1999). *Genes Dev.*, **13,** 2604–2616.

Clevenger CV, Furth PA, Hankinson SE and Schuler LA. (2003). *Endocr. Rev.*, **24,** 1–27.

Cotarla I, Ren S, Zhang Y, Gehan E, Singh B and Furth PA. (2004). *Int. J. Cancer*, **108,** 665–671.

Coussens LM and Werb Z. (1996). *Chem. Biol.*, **3,** 895–904.

Das R and Vonderhaar BK. (1996). *Oncogene*, **13,** 1139–1145.

Duhe RJ, Rui H, Greenwood JD, Garvey K and Farrar WL. (1995). *Gene*, **158,** 281–285.

Erwin RA, Kirken RA, Malabarba MG, Farrar WL and Rui H. (1995). *Endocrinology*, **136,** 3512–3518.

Fearon ER. (2003). *Cancer Cell*, **3,** 307–310.

Gouilleux F, Wakao H, Mundt M and Groner B. (1994). *EMBO J.*, **13,** 4361–4369.

Grimley PM, Dong F and Rui H. (1999). *Cytokine Growth Factor Rev.*, **10,** 131–157.

Groner B and Hennighausen L. (2000). *Breast Cancer Res.*, **2,** 149–153.

Humphreys RC and Hennighausen L. (1999). *Cell Growth Differ.*, **10,** 685–694.

Iavnilovitch E, Groner B and Barash I. (2002). *Mol. Cancer Res.*, **1,** 32–47.

Kabotyanski EB and Rosen JM. (2003). *J. Biol. Chem.*, **278,** 17218–17227.

Kazansky AV, Raught B, Lindsey SM, Wang YF and Rosen JM. (1995). *Mol. Endocrinol.*, **9,** 1598–1609.

Kemler R and Ozawa M. (1989). *BioEssays*, **11,** 88–91.

Kim J, Yu W, Kovalski K and Ossowski L. (1998). *Cell*, **94,** 353–362.

Kinch MS, Clark GJ, Der CJ and Burridge K. (1995). *J. Cell Biol.*, **130,** 461–471.

Le TL, Yap AS and Stow JL. (1999). *J. Cell Biol.*, **146,** 219–232.

Lilien J, Balsamo J, Arregui C and Xu G. (2002). *Dev. Dyn.*, **224,** 18–29.

Liu X, Gallego MI, Smith GH, Robinson GW and Hennighausen L. (1998). *Cell Growth Differ.*, **9,** 795–803.

Liu X, Robinson GW, Gouilleux F, Groner B and Hennighausen L. (1995). *Proc. Natl. Acad. Sci. USA*, **92,** 8831–8835.

Liu X, Robinson GW and Hennighausen L. (1996). *Mol. Endocrinol.*, **10,** 1496–1506.

Liu X, Robinson GW, Wagner KU, Garrett L, Wynshaw-Boris A and Hennighausen L. (1997). *Genes Dev.*, **11,** 179–186.

Marte BM, Jeschke M, Graus-Porta D, Taverna D, Hofer P, Groner B, Yarden Y and Hynes NE. (1995). *Mol. Endocrinol.*, **9,** 14–23.

Maus MV, Reilly SC and Clevenger CV. (1999). *Endocrinology*, **140,** 5447–5450.

Mbalaviele G, Dunstan CR, Sasaki A, Williams PJ, Mundy GR and Yoneda T. (1996). *Cancer Res.*, **56,** 4063–4070.

Miyoshi K, Shillingford JM, Smith GH, Grimm SL, Wagner KU, Oka T, Rosen JM, Robinson GW and Hennighausen L. (2001). *J. Cell Biol.*, **155,** 531–542.

Nevalainen MT, Xie J, Bubendorf L, Wagner KU and Rui H. (2002). *Mol. Endocrinol.*, **16,** 1108–1124.

Nevalainen MT, Xie J, Torhorst J, Bubendorf L, Haas P, Kononen J, Sauter G and Rui H. (2004). *J. Clin. Oncol.*, **22,** 2053–2060.

Papkoff J. (1997). *J. Biol. Chem.*, **272,** 4536–4543.

Paterson AD, Parton RG, Ferguson C, Stow JL and Yap AS. (2003). *J. Biol. Chem.*, **278,** 21050–21057.
Philips N and McFadden K. (2004). *Cancer Lett.*, **206,** 63–68.
Ren S, Cai HR, Li M and Furth PA. (2002). *Oncogene*, **21,** 4335–4339.
Schaber JD, Fang H, Xu J, Grimley PM and Rui H. (1998). *Cancer Res.*, **58,** 1914–1919.
Schmidhauser C, Casperson GF, Myers CA, Sanzo KT, Bolten S and Bissell MJ. (1992). *Mol. Biol. Cell*, **3,** 699–709.
Shiu RP and Paterson JA. (1984). *Cancer Res.*, **44,** 1178–1186.
Stockinger A, Eger A, Wolf J, Beug H and Foisner R. (2001). *J. Cell Biol.*, **154,** 1185–1196.
Sultan AS, Miyoshi E, Ihara Y, Nishikawa A, Tsukada Y and Taniguchi N. (1997). *J. Biol. Chem.*, **272,** 2866–2872.
Teglund S, McKay C, Schuetz E, van Deursen JM, Stravopodis D, Wang D, Brown M, Bodner S, Grosveld G and Ihle JN. (1998). *Cell*, **93,** 841–850.
Udy GB, Towers RP, Snell RG, Wilkins RJ, Park SH, Ram PA, Waxman DJ and Davey HW. (1997). *Proc. Natl. Acad. Sci. USA*, **94,** 7239–7244.
Wagner K-U, Krempler A, Triplett AA, Qi Y, George NM, Zhu J and Rui H. (2004). *Mol. Cell Biol.*, **24,** 5510–5520.
Wakao H, Gouilleux F and Groner B. (1994). *EMBO J.*, **13,** 2182–2191.
Wheelock MJ and Johnson KR. (2003). *Annu. Rev. Cell Dev. Biol.*, **19,** 207–235.
Xie J, LeBaron MJ, Nevalainen MT and Rui H. (2002). *J. Biol. Chem.*, **277,** 14020–14030.
Yamashita H, Iwase H, Toyama T and Fujii Y. (2003). *Oncogene*, **22,** 1638–1652.
Yamashita H, Xu J, Erwin RA, Larner AC and Rui H. (1999). *J. Biol. Chem.*, **274,** 14699–14705.
Yasumitsu H, Miyazaki K, Umenishi F, Koshikawa N and Umeda M. (1992). *J. Biochem. (Tokyo)*, **111,** 74–80.
Zhang S, Herrmann C and Grosse F. (1999). *J. Cell Sci.*, **112** (Part 16), 2693–2703.